tektonika

# The Saxo-Thuringian Basin of the Central European Variscides: Subsurface Characterization of a Lateral Foreland Basin Based on an Integrated Geophysical Data Set

**Hamed Fazlikhani** [*1], **Uwe Kroner** [2], **Harald Stollhofen** [1], **Wolfgang Bauer**[1], **Daniel Koehn** [1]

[1]Friedrich-Alexander-Universität (FAU) Erlangen-Nürnberg, GeoZentrum Nordbayern, Erlangen, Schlossgarten 5, 91054 Erlangen, Germany | [2]Department of Geology, TU Bergakademie Freiberg, B.-v.-Cotta-Strasse 2, D-09596 Freiberg, Germany

**Abstract** The lateral extent of subsurface structures and lithologies of ancient orogenies are frequently obscured by younger units, which restricts our understanding of orogenic processes. In these regions, subsurface characterization can be conducted through the integration, interpretation, and modelling of geophysical and geological data. In this case study, we examine the lateral extent of the Variscan Saxo-Thuringian Basin, which formed during the early Carboniferous and is partly exposed in the NW Bohemian Massif. West of the Bohemian Massif, the architecture of the entire Saxo-Thuringian Basin and surrounding basement units remain elusive due to the complete coverage by post-Variscan sedimentary rocks. The low magnetic field intensity signature of the exposed portion of the Saxo-Thuringian Basin, in combination with information from basement drilled wells and observed seismic reflection facies, is used to define the western extent of the basin covered by Permian-Mesozoic units. Integrated geological and geophysical data interpretation and modelling show the geometry of the Saxo-Thuringian Basin as a 60 km long and 60 km wide area west of the Bohemian Massif. Regional Bouguer gravity anomalies are related to the folding and thrusting of basement rocks and emplacement of orogenic granites, while local anomalies are interpreted as Permian fault-bounded graben and half-graben structures. The Saxo-Thuringian Basin is developed in an upper plate position as part of a strike-slip dominated segment of the Gondwana-Laurussia plate boundary zone on a "low-strain" zone. Due to its lateral position relative to the collisional pile of the Bohemian Massif, we define it as a "lateral foreland" basin.

Executive Editor:
**Graeme Eagles**
Associate Editor:
**Hongdan Deng**
Technical Editor:
**Mohamed Gouiza**

Reviewers:
**Wolfram Geissler**
**Anonymous Reviewer**

Submitted:
**22 July 2024**
Accepted:
**5 May 2025**
Published:
**14 July 2025**

## 1 Introduction

A detailed knowledge of the architecture of continental crust is essential for the analysis of orogenic processes. In the context of geodynamic models, it is important to consider the limited availability of geological constraints at the regional scale. The orogenic crust, in a state of thermal and gravitational equilibrium, is characterized by a flat topography and is often overlaid by post-orogenic sedimentary rocks. In such a case, integration of the geophysical data sets and the information obtained from wells can be used. The combination of geophysical data set and information from wells with available constraints derived from exposed orogenic crust of the area represents the optimal approach for regional studies, as it allows for a more comprehensive understanding of the area in question.

The Saxo-Thuringian Zone of the Central European Variscides (*Kossmat*, 1927) provides an illustrative case study for this approach. The basement rocks have been consolidated in the late Palaeozoic and subsequently covered by post-orogenic lithologies. Late Mesozoic to Cenozoic intraplate tectonics (*Kley and Voigt*, 2008) have resulted in the recent juxtaposition of pre-Mesozoic units and younger lithologies in the northeast and the southwest respectively, which are separated by the NW-SE striking Franconian Fault System (Figure 1). The exposed part of the Saxo-Thuringian lithologies display a great complexity comprising very low grade pre- and synorogenic sediments in tectonic contact with medium to high grade allochthonous complexes. The crystalline units partly experienced Variscan (ultra) high pressure (*Massonne*, 1998; *Rötzler and Plessen*, 2010; *Schmädicke et al.*, 1992; *Willner et al.*, 2000), as well as ultra-high temperature (*Reinhardt and Kleemann*, 1994; *Rötzler and Romer*, 2001) metamorphism indicating continental subduction until the early Carboniferous (~340 Ma, e.g., *Kröner et al.*, 1998; *Kylander-Clark et al.*, 2013) and rapid exhumation in upper crustal levels until 330 Ma (*Hallas et al.*, 2021; *Rötzler and Romer*, 2001). Most importantly, the tectono-metamorphic evolution of the Saxo-Thuringian crystalline complexes

*✉ hamed.fazlikhani@gmail.com

occurred contemporaneous with marine sedimentation in the synorogenic Saxo-Thuringian Basin (STB, *Hahn et al.*, 2010).

Consequently, tectonic models changed significantly from the traditional view of (*Kossmat*, 1927) and also from first plate tectonic explanations (*Franke*, 1989). Traditionally the entire Saxo-Thuringian Zone (STZ) has been regarded as a long-lived marine basin that was characterized by continuous sedimentation onto a Precambrian basement from the Neoproterozoic until the early Carboniferous (*von Gaertner*, 1951). Hence, the term Saxo-Thuringian Basin (STB) has been assigned as a synonym for the entire Saxo-Thuringian Zone. In such a view, the Neoproterozoic / Palaeozoic lithologies of the so called (par)autochthonous "Thuringian facies" are overlain by the allochthonous sequences of the exotic "Bavarian Facies". Synorogenic sedimentation commenced in the early Carboniferous and lasted from upper Tournaisian to upper Visean times (e.g., *Falk et al.*, 1995). Due to late Variscan NW-SE convergence the entire STB is folded, and in the SE, the (meta)-sedimentary pile is overthrusted by the crystalline complex of the Münchberg nappe as part of the Moldanubian Zone (*Franke*, 1984a; *Wurm*, 1926).

In a plate tectonic perspective of the Variscan Orogeny (*Matte*, 1986), the entire STZ has been reinterpreted as a microplate that was separated from the Moldanubian microplate by the long-lived Saxo-Thuringian Ocean (e.g., *Franke et al.*, 1995). The subduction of the oceanic lithosphere was eventually followed by the frontal collision with the Moldanubian microplate causing the Variscan Orogeny (*Franke et al.*, 1995). Prolonged NW-SE convergence affected the STB changing from a narrow marine basin to a NE-SW striking early Carboniferous flexural foreland basin in front of NW-ward stacking Moldanubian units in the SE and at the same time as a hinterland basin to the Rheno-Hercynian Zone to the NW (*Franke et al.*, 1995; *Krawczyk et al.*, 2000; *Oncken*, 1998). The final architecture is characterized by nearly cylindrical, NE-SW striking synclines and anticlines resembling the tectonic model of (*Wurm*, 1926).

In contrast to an exclusive NW-SE convergence of various microplates, *Kroner et al.* (2007) explain the STZ as a remnant of the Gondwana plate in a generic two plate scenario of the Variscan Orogeny (*Kroner and Romer*, 2013). Deduced from early Variscan pervasive nappe tectonics, for Central Europe, the proposed Gondwana–Laurussia plate convergence is NE-SW which is perpendicular to the traditional view of exclusive NW-SE shortening. In such a view, the Mid German Crystalline Zone represents the remnant of a sinistral strike slip plate-boundary zone (*Stephan et al.*, 2016). Late Variscan NNW-SSE sinistral transpression due to orogen-wide tectonic reorganization finally affected also the STZ (*Stephan et al.*, 2019). Thus, the exclusive NW-SE compression proposed by the traditional models is explained as the latest Variscan deformation phase overprinting a heterogeneously deformed continental crust.

Because the deposition of the youngest synorogenic sediments postdates the early Variscan tectonics the NNW-SSE compression only affected the central parts of the STB. The general architecture of the synorogenic STB, however, remains elusive due to the complete coverage by post-Variscan sedimentary rocks SW of the Franconian Fault System (FFS, Figure 1). To define the lateral extent of the entire STB and characterize surrounding basement rocks, we concentrate on the lower Carboniferous turbiditic deposits exposed in the NW part of the Bohemian Massif and its SW extension across the FFS. We use an integrated methodology based on geophysical (gravity, magnetic and seismic reflection) and geological (surface geology and well) data and gravity modelling to propose the W-SW boundary of the synorogenic STB. We show, that the basin evolution is not in conflict with a strike slip dominated segment of the Gondwana – Laurussia plate boundary zone. We define the STB as a lateral foreland basin accreted during the ongoing Gondwana – Laurussia collision. Furthermore, we discuss implications for the central European Variscan tectonics and the importance of data integration and modelling in subsurface characterization.

## 2 Geological Setting

The STB contains >3600 m of early Carboniferous (upper Tournaisian-upper Visean ∼350-334 Ma) distal and proximal turbidites (*Falk et al.*, 1995; *Hahn et al.*, 2010). These turbidites overlay shelf sediments deposited from the Cambrian onwards (*Linnemann et al.*, 2004; *Robardet*, 2002). Prior to the synorogenic sedimentation, the open marine environment can be subdivided into an inner and an outer shelf facies equivalent to the traditional terms "Thuringian" and "Bavarian" facies of (*Wurm*, 1926, 1961). The pre-Variscan marine sediments represent remnants of a vast passive continental margin south of the Rheic Ocean. The ages of detrital zircons reveal West-African provenance (*Linnemann et al.*, 2004; *Stephan et al.*, 2019). In the SE of the STZ, the metasediments of the Variscan Erzgebirge-Fichtelgebirge Zone represent pervasively deformed and metamorphosed latest Proterozoic to early Palaeozoic protoliths comparable to the very low grade lithologies exposed in the NW of the STZ (*Mingram*, 1998; *Romer and Kroner*, 2022; *Tichomirowa et al.*, 2012). The tectono-metamorphic record of the Erzgebirge-Fichtelgebirge Zone reveals prolonged subduction-, accretion-, exhumation-processes lasting from the early Devonian until the early Carboniferous (*Hallas et al.*, 2021; *Jouvent et al.*, 2022; *Romer et al.*, 2022; *Rötzler and Plessen*, 2010; *Willner et al.*, 2000). The pervasive deformation (>340 Ma) of the allochthonous units is related to initial SW-directed nappe stacking (*Kroner et al.*, 2007). It is noteworthy that the subduction accretion processes in the allochthonous Erzgebirge-Fichtelgebirge Zone and the uppermost allochthonous Münchberg nappe (gneiss complex) occurred synchronous to continuous marine sedimentation in the Autochthonous Domain of the STZ (*Kroner et al.*, 2007). To the NW, the STZ is bounded by the Mid-German Crystalline Zone, exposing medium

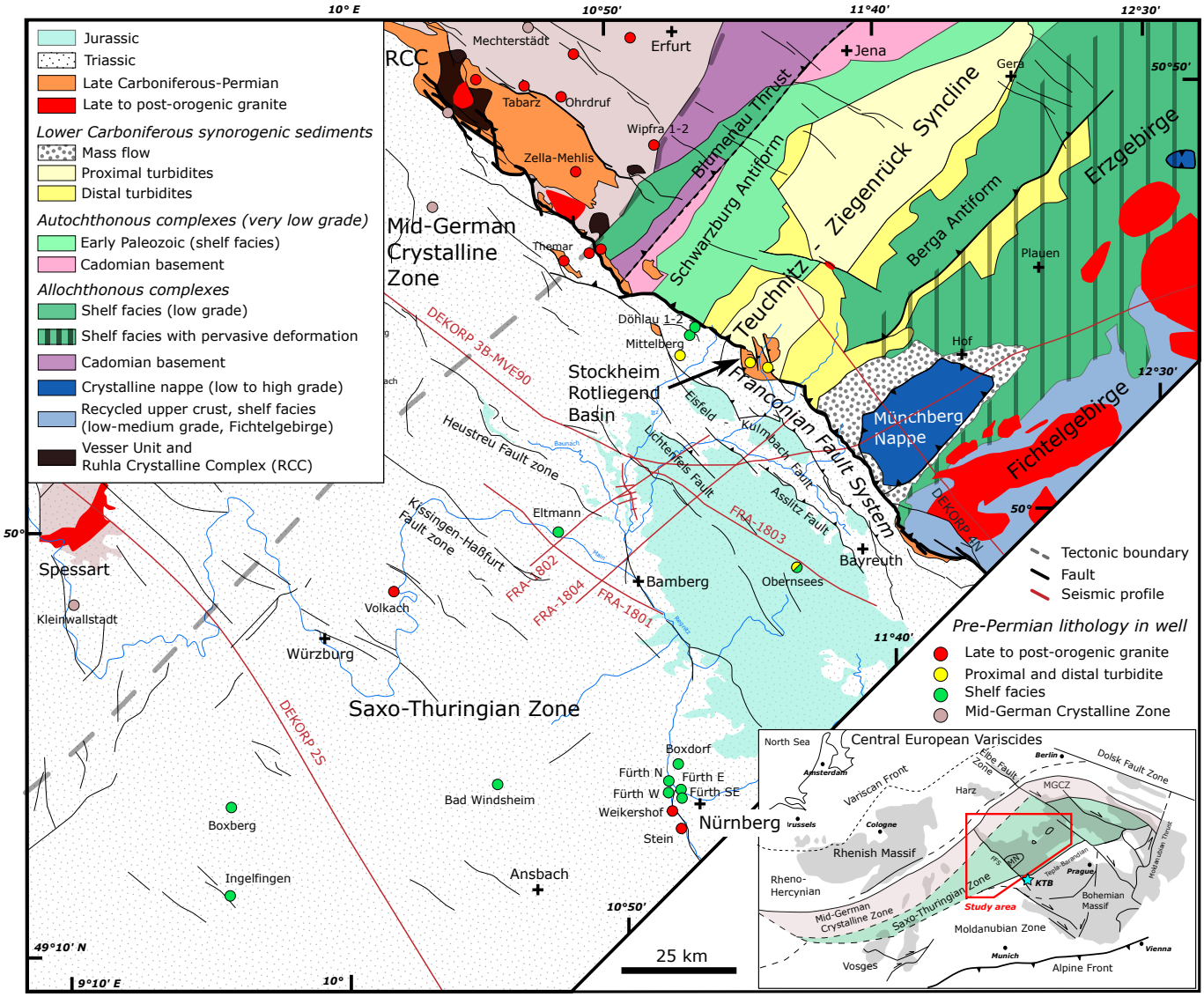


**Figure 1** – Study area in the NW Bohemian Massif and the Franconian Platform on the east and west sides of the Franconian Fault System (FFS). Inset map shows the major tectonostratigraphic and structural elements of the Central European Variscides and the study area; the Saxo-Thuringian Zone is highlighted. West of the FFS basement wells are colour-coded according to the rock types exposed east of the FFS. Note that the two circles west of the Teuchnitz-Ziegenrück Syncline represent six closely located wells: Wolfersdorf, Wolfersdorf E, Wolfersdorf S, Reitsch N, Stockheim SSW, and Burggrub NNE, see Table 1 for well information. Bohemian Massif units are based on (*Linnemann*, 2007), tectono-stratigraphic units based on (*Kroner et al.*, 2007) and faults and Mesozoic units based on Geological map of Germany 1:500,000.

and high-grade rocks and late- to post- Variscan granitic intrusions (*Zeh and Will*, 2010). The Mid-German Crystalline Zone is dominated by the NE-trending sinistral strike-slip shear zones documented along the exposed crystalline rocks e.g. in the Odenwald and Ruhla crystalline complexes (*Krohe*, 1992; *Wunderlich*, 1989; *Zeh and Will*, 2010). The deformation of the Mid-German Crystalline zone terminated by ca. 335 Ma. and it is almost unaffected by the late Variscan tectonics (*Krohe*, 1992; *Scherer et al.*, 2002; *Stephan et al.*, 2016; *Will*, 2001; *Will et al.*, 2021).

For the synorogenic sediments detailed mapping by *Hahn et al.* (2010) along the Teuschnitz-Ziegenrück Syncline led to a subdivision of three principal stages in the development of the STB: i) orogenic foreland stage, ii) main deformation phase at ca. 340 Ma affecting the SE-part of the synorogenic sediments coeval with the main deformation event in the Allochthonous Domain (*Kroner et al.*, 2007) of the STZ; iii) the overfill stage in the late Visean that terminated at ca. 334 Ma. Synorogenic sedimentation commenced in the upper Tournaisian (*Franke*, 1984b; *Gandl*, 1998) and is characterized as distal turbidites at ca. 360 Ma. (*Hahn et al.*, 2010). These distal turbidites intercalate with pelites and sapropelites of the inner shelf facies (Figure 2A). At ca. 342 Ma the entire STB is covered by the distal turbidites with coarser units next to the SE margin of the basin (*Falk et al.*, 1995; *Kroner et al.*, 2007). As indicated by stretching lineation and shear sense indicators (*Hahn et al.*, 2010; *Kroner et al.*, 2007), SW-directed thrusting and nappe transport affected the SE edge of the STB (during stage ii) and is coeval with the final nappe stacking in the adjacent allochthonous domain. The overfill stage of the STB started at ca. 340 Ma and is related to the NW directed deposition

of voluminous mass flow units (wildflysch) in the SE (Figure 2C). These proximal successions form a NE-SW trending belt and define the SE border of the STB. More distal axial turbiditic currents in the NW are indicative of a narrow, NE-SW synorogenic basin during the overfill stage (*Hahn et al.*, 2010). With the deposition of voluminous proximal siliciclastic sediments in the central parts of the basin, marine sedimentation ceased, and the entire succession was subjected to late Variscan compressional tectonics and deformation (Figure 2D).

Final NW-SE compression of the Variscan tectonics resulted in SE-vergent folding in the central parts of the STB. Whereas the allochthonous units of the STZ display a complex deformation pattern, synorogenic sediments deposited after initial nappe stacking experienced exclusively late Visean NW–SE shortening as for example evidenced by the uppermost lithologies of the Teuschnitz-Ziegenrück Syncline. SW of the exposed parts of the STB and across the FFS, post-Variscan Permo-Mesozoic deposits cover the metamorphic basement of the STZ and possible turbidity infill of the STB (Figure 1).

# 3 Data and Methods

## 3.1 Potential Field, Seismic Reflection and Well Data

Total magnetic field intensity grid, Bouguer gravity anomaly grid, seismic reflection and wells penetrating pre-Permian basement form the dataset used in this study. Geophysical data are particularly useful in identifying gravity and magnetic anomalies and reflection patterns related to the STB exposed in the NW of the Bohemian Massif. Where the STB is covered by the Permian-Mesozoic rocks, geophysical data in combination with the pre-Permian basement wells are used in defining the SW extension of the STB (Table 1 and Figure 1). The compiled total magnetic field anomaly dataset is based on 67 ground and airborne surveys that has a grid spacing of 100 meters and a common reference level of 1000 m altitude (for more details on magnetic data compilation and processing see *Gabriel et al.*, 2011). The Bouguer gravity anomaly map is based on 275,000 gravimetry points with an average point separation of 2-3 km, compiled and processed by the Leibniz Institute for Applied Geophysics (*Skiba et al.*, 2010). Seismic reflection data comprise the reprocessed DEKORP 3B-MVE90 and 4N profiles imaging the exposed and buried Variscan units across the FFS (*DEKORP Research Group*, 1988, 1994a; *Fazlikhani et al.*, 2022). The Permian-Mesozoic cover and the SW extension of Variscan units including the STB west of FFS are best imaged by the FRANKEN seismic survey and the pre-Permian wells in northern Bavaria (*DEKORP Research Group*, 1988, 1994a; *Fazlikhani et al.*, 2022).

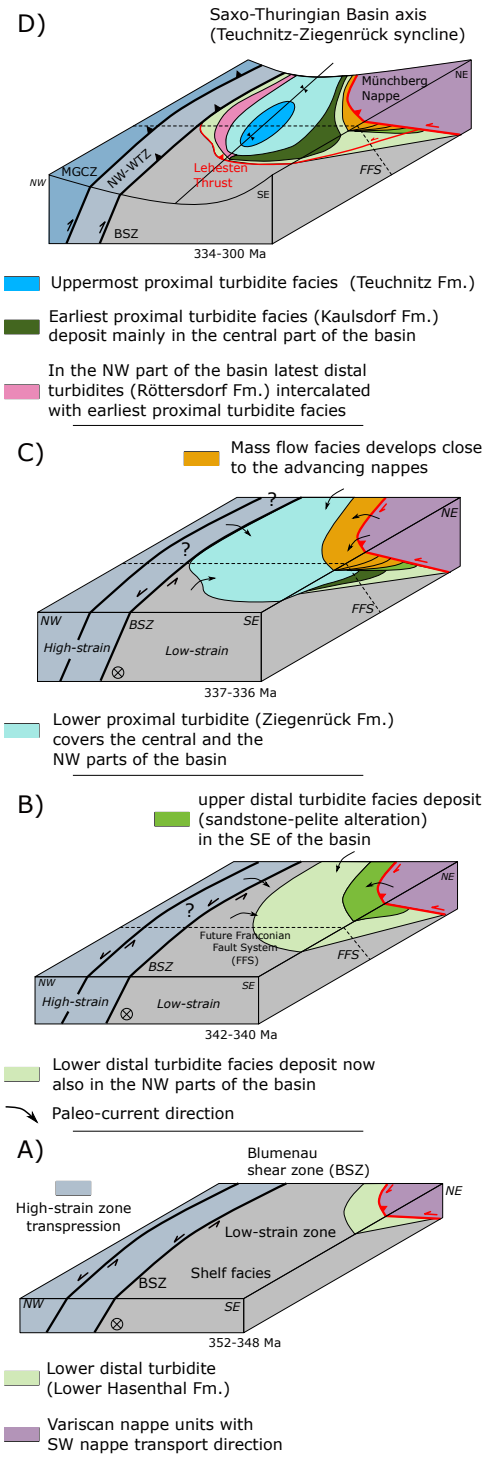


**Figure 2** – Schematic cartoons showing temporal development of the Saxo-Thuringian Basin (STB) from the early distal turbidites deposition at 352 Ma **(A)** based on detailed mapping of (*Hahn et al.*, 2010). The SE parts of the STB first receive the distal turbidites while the central and NW parts are still in a shelf environment. Progressive facies change occurring from the SE to the NW of the STB reflects the main deformation front in the SE **(B & C)**. After 334 Ma **(D)** previous strike-slip shear zones reactivate as thrust shear zone (e.g., Blumenau shear zone; *Stephan et al.*, 2016) along with a new generation of thrust zone such as the Lehesten thrust (D, at ca. 320 Ma; *Schäfer et al.*, 2000). MGCZ: Mid German Crystalline Zone, BSZ: Blumenau Shear Zone, FFS: Franconian Fault System, NW-WTZ: Northwest Wrench and Thrust Zone (*Kroner et al.*, 2007).

**Table 1** – List of wells drilled into basement shown in the Figures 1.

| Well | Drilled basement units and references |
|---|---|
| Buchenau A6/40 | Proterozoic, Mid-German Crystalline Zone, *Richter* (1941) |
| Mechterstädt 1/62 | Proterozoic, Mid-German Crystalline Zone, *Richter* (1941) |
| Krahnberg 3/64 | Proterozoic, Mid-German Crystalline Zone, *Brosin and Lützner* (2012) |
| Sprötau 3/63 | Proterozoic, Mid-German Crystalline Zone, *Brosin and Lützner* (2012) |
| Neudietendorf 3/62 | Proterozoic, Mid-German Crystalline Zone, *Brosin and Lützner* (2012) |
| Liebenstein | Proterozoic, Mid-German Crystalline Zone, *Reh* (1954) |
| Oberkatz | Proterozoic, Mid-German Crystalline Zone, *Andreas* (2013) |
| Waldberg | Proterozoic, Mid-German Crystalline Zone, Bavarian Environment Agency (LfU) (see Appendix B in Supporting Information) |
| Geroda | Proterozoic, Mid-German Crystalline Zone, Bavarian Environment Agency (LfU) (see Appendix B in Supporting Information) |
| Kleinbrach | Late Variscan granite, Bavarian Environment Agency (LfU) (see Appendix B in Supporting Information) |
| Gotha 1/63 | Late Variscan granite (Thüringer Hauptgranit), *Brosin and Lützner* (2012) |
| Ohrdruf | Late Variscan granite (Thüringer Hauptgranit), *Andreas* (2013) |
| Tabarz | Late Variscan granite (Thüringer Hauptgranit), *Andreas* (2013) |
| Volkach | Pre-Variscan granite (Ordovician syenite), *Eckhardt* (1962); *Anthes and Reischmann* (2001) |
| Weikershof | Late Variscan granite, *Wurm* (1929) |
| Stein | Late Variscan granite, *Wurm* (1929) |
| Wipfra 1/62 | Late Variscan granodiorite, *Ziegenhardt and Jungwirth* (1972) |
| Wipfra 2/63 | Late Variscan granodiorite, *Ziegenhardt and Jungwirth* (1972) |
| Themar 1/1963 | Late Variscan granite (Thüringer Hauptgranit), *Judersleben* (1972) |
| Schleusingen 3/64 | Late Variscan granodiorite (Thüringer Hauptgranit), *Schust et al.* (2000) |
| Schleusingen 1/63 | Late Variscan granodiorite (Thüringer Hauptgranit), *Andreas* (2013) |
| Zella-Mehlis 1/1964 | Late Variscan granite (Thüringer Hauptgranit), *Andreas et al.* (1975) |
| Wolfersdorf | Lower Carboniferous (lower Proximal turbidites, Ziegenrück Fm.), Bavarian Environment Agency (LfU) (see Appendix B in Supporting Information) |
| Wolfersdorf E | Lower Carboniferous (lower Proximal turbidites, Ziegenrück Fm.), Bavarian Environment Agency (LfU) (see Appendix B in Supporting Information) |
| Wolfersdorf S | Lower Carboniferous (lower Proximal turbidites, Ziegenrück Fm.), Bavarian Environment Agency (LfU) (see Appendix B in Supporting Information) |
| Reitsch N | Lower Carboniferous (lower Proximal turbidites, Ziegenrück Fm.), Bavarian Environment Agency (LfU) (see Appendix B in Supporting Information) |
| Stockheim SSW | Lower Carboniferous (lower Proximal turbidites, Ziegenrück Fm.), Bavarian Environment Agency (LfU) (see Appendix B in Supporting Information) |
| Burggrub NNE | Lower Carboniferous (lower Proximal turbidites, Ziegenrück Fm.), Bavarian Environment Agency (LfU) (see Appendix B in Supporting Information) |
| Mittelberg | Uppermost Devonian-lower Carboniferous turbidites, *Trusheim* (1964) |
| Obernsees | Lower Carboniferous turbidites, Bavarian Environment Agency (LfU) (see Appendix B in Supporting Information)<br>Devonian metasediments (inner shelf facies), *Stettner and Salger* (1985) |
| Bad Windsheim SE | Cambrian-lower Carboniferous (Inner shelf facies to outer shelf facies), *Linnemann et al.* (2010) |
| Eltmann | Devonian metasediments (inner shelf facies), *Trusheim* (1964) |
| Boxdorf | Devonian Inner shelf facies, *Wurm* (1929) |
| Fürth N (Bremenstall) | Devonian Inner shelf facies, *Wurm* (1929) |
| Fürth N (Poppenreuth) | Devonian Inner shelf facies, *Wurm* (1929) |
| Fürth W (TH 1/2004) | Upper Ordovician Inner shelf facies, *Wurm* (1929) |
| Fürth SE (Espan) | Devonian-Carboniferous Inner shelf facies, *Wurm* (1929) |
| Döhlau 1/63 | Cambrian-lower Carboniferous inner shelf facies, *Andreas* (2013) |
| Döhlau 2/64 | Cambrian-lower Carboniferous inner shelf facies, *Andreas* (2013) |
| Boxberg | Ordovician? inner shelf facies, *Stamm and Goerlich* (1988) |
| Ingelfingen | Devonian-Carboniferous? inner shelf facies, *Stamm and Goerlich* (1988) |

## 3.2 Rock Sampling and Density Measurement

In order to build a rock density database that better reflects the local geology we sampled representative rocks and measured densities in our laboratory. Our dataset is compared and completed with the published datasets (*Bosum et al.*, 1997; *Hofmann*, 2003; *Hofmann et al.*, 2003; *de Wall et al.*, 2019). Densities are measured on 30 mm diameter and 10-40 mm long plugs obtained from sampled rocks. Samples were dried at 60°C for 48 hours and then stored at room temperature prior to density measurements. Bulk density measurements were carried out using a Micromeritics GeoPyc device that automatically determines the volume and density of a solid object by displacement of a solid medium. We applied a 10 measurement cycles mode to each sample and then calculated the average of 10 measurements, listed in Table 2. After defining the initial subsurface unit geometry based on the seismic reflection interpretation, and density values attributed to each unit, the interactive modelling has been done until the best fit between the measured and modeled gravity anomalies has been achieved. Rock densities used in forward gravity models are assumed constant vertically and horizontally within each model unit. Forward models are constructed using the commercial GM-SYS (Seequent) software which is an interactive gravity and magnetic modelling tool that uses a method of summing the effects of irregular polygons (*Talwani*, 1973).

## 3.3 Forward Gravity Modelling

West of the FFS, where the Variscan units are covered by Permian-Mesozoic sedimentary rocks, we integrate surface geology, well and gravity data and construct two 2D forward gravity models parallel to the seismic reflection profile FRANKEN 1802 and the composite FRANKEN 1803/DEKORP 3B-MVE90 profiles. Potential field data produce non-unique 2D models in a way that various subsurface configurations can result in the same amplitude and wavelength anomaly. In addition, 2D modelling of gridded gravity data could be influenced by the causative bodies or features that are out of the plane of the modeled profile. In order to increase confidence in our 2D models, the geometry and the thickness of the Mesozoic units down to the top of the Permian, as well as the major faults are constrained based on the interpretation of the seismic reflection data tied to the wells (see Table 3 for the Permian and Mesozoic lithologies from wells). The geometry and the thickness of the middle and lower crustal units and the Moho discontinuity are constrained based on the seismic refraction and reflection studies (*DEKORP Research Group*, 1994a,b; *Enderle et al.*, 1998; *Schulmann et al.*, 2022). By constraining the thickness and the geometry of the sedimentary cover, middle and lower crust, and the Moho discontinuity based on the published surface geology, well, seismic reflection and refraction data, the main uncertainties in our forward models are the architecture and distribution of Carboniferous-Permian (Rotliegend) basins, the STB

**Table 2** – Rock density values measured on outcrop samples and well cores, used in forward gravity modelling.

| | Sample (outcrop/well core) | Stratigraphy | Bulk Density | Reference |
|---|---|---|---|---|
| Tertiary Baslat | Outcrop sample | | 3096 | This study |
| Jurassic | Well Obernsees | | 2400 | *De Wall and Stollhofen* (2016, 2017) |
| Triassic | Wells Obernsees and Mürsbach 1 +outcrop sample | Keuper | 2225 | *De Wall and Stollhofen* (2016, 2017) |
| | | Muschelkalk | 2633 | *De Wall and Stollhofen* (2016, 2017) |
| | | Buntsandstein | 2286 | *De Wall and Stollhofen* (2016, 2017) |
| Zechstein | Well Obernsees | Zechstein | 2458 | *De Wall and Stollhofen* (2016, 2017) |
| | Well Mürsbach1 +outcrop sample | Zechstein | 2798 | *De Wall and Stollhofen* (2016, 2017) |
| | Well Lindau1 | Zechstein | 2300 | *Ravidà* (2023) |
| | Well Neuenbuch1 | Zechstein | 2520 | *Ravidà* (2023) |
| Rotliegend | Well Obernsees | Rotliegend | 2537 | *De Wall and Stollhofen* (2016, 2017) |
| | Well Mürsbach1 +outcrop sample | Rotliegend | 2613 | *De Wall and Stollhofen* (2016, 2017) |
| | Well Lindau1 | Rotliegend | 2430 | *Ravidà* (2023) |
| | Well Neuenbuch1 | Rotliegend | 2510 | *Ravidà* (2023) |
| | Outcrop sample | Rotliegend (Erbendorf Basin) | 2616 | This study |
| | Outcrop sample | Rotliegend (Weidenberg) | 2670 | This study |
| | Outcrop sample | Rotliegend (Stockheim Fm.) | 2279 | This study |
| | Outcrop sample | Rotliegend (Stockheim, Reitsch Fm) | 2289 | This study |
| Lower Carboniferous turbidite | Outcrop sample | Lower Carboniferous Mass Flow | 2710 | This study |
| | Outcrop sample | Lower Carboniferous Teuschnitz Fm. | 2417 | This study |
| | Outcrop sample | Lower Carboniferous Teuschnitz Fm. | 2559 | This study |
| | Outcrop sample | Lower Carboniferous Teuschnitz Fm. | 2608 | This study |
| | Outcrop sample | Lower Carboniferous Teuschnitz Fm. Graywack conglomerat | 2619 | This study |
| | Outcrop sample | Lower Carboniferous Teuschnitz Fm. Graywack | 2381 | This study |
| | Outcrop sample | Lower Carboniferous Ziegenrück Fm. | 2690 | This study |
| | Outcrop sample | Lower Carboniferous Leutenberg Gr. Röttersdorf Fm. | 2465 | This study |
| | Outcrop sample | Lower Carboniferous Leutenberg Gr. Kaulsdorf Fm | 2326 | This study |
| | Outcrop sample | Lower Carboniferous Leutenberg Gr. Hasenthal Fm | 2631 | This study |
| | Outcrop sample | Lower Carboniferous Leutenberg Gr. Lehesten Fm. | 2599 | This study |
| | Outcrop sample | Lower Carboniferous Russschiefer Fm. | 2739 | This study |
| Devonian | Outcrop sample | U.Dev-L.Carb_Saalfeld Gr. Gleitsch Fm. | 2791 | This study |
| | Outcrop sample | U.Dev_Saalfeld Gr. Bohlem Fm. | 2780 | This study |
| | Outcrop sample | U.Dev_Saalfeld Gr. Görkwitz-Fm. | 2398 | This study |
| | Outcrop sample | M.Dev_Schwärzschiefer-Fm. | 2558 | This study |
| | Outcrop sample | L.Dev (Emsian)_Tentakuliten-schiefer-Fm. | 2578 | This study |
| | Outcrop sample | L.Dev (Pragian)_Tentakuliten-knollenkalk-Fm. | 2755 | This study |
| Silurian | Outcrop sample | U.Sil-L.Dev_Obere Graptolithen-schiefer-Fm. | 2751 | This study |
| | Outcrop sample | U.Sil_Ockerkalk-Fm. | 2689 | This study |
| | Outcrop sample | L.Sil. (Llandovery) Untere Graptolithen-schiefer-Fm. | 2550 | This study |
| Ordovician | Outcrop sample | U.Ord. (ashgill)_Gräfenthal Gr._Lederschiefer-Fm. | 2682 | This study |
| | Outcrop sample | U.Ord. (ashgill)_Gräfenthal Gr._Hauptquarzit-Fm. | 2427 | This study |
| | Outcrop sample | U.Ord. (ashgill)_Gräfenthal Gr._Schmiedefeld-Fm. | 2640 | This study |
| | Outcrop sample | U.Ord._Gräfenthal Gr.Griffelschiefer-Fm. | 2808 | This study |
| | Outcrop sample | L.Ord._Phycodes Gr. Phycodenquarzit-Fm. | 2682 | This study |
| | Outcrop sample | L.Ord._Phycodes Gr. Phycodenschiefer-Fm. | 2395 | This study |
| | Outcrop sample | L.Ord._Frauenbach Gr. | 2456 | This study |

(lower Carboniferous turbidites), the location of possible late Variscan granitic intrusions, and deeper parts of the upper crust. Depth conversion of interpreted unit boundaries and thicknesses were conducted using sonic log data, and published seismic velocity models (*Enderle et al.*, 1998; *Fazlikhani et al.*, 2022). The Moho discontinuity is imaged along the DEKORP profiles and is modeled between 28-32 km which is in accordance with published Moho depth maps of western Europe (*Schulmann et al.*, 2022).

# 4 Interpretation and Modelling Results

## 4.1 Seismic Reflection and Well Data

Seismic profile DEKORP 3B-MVE90 images Variscan allochthons and the Franconian Platform across the FFS (Figure 3A and B). West of the FFS strong and continuous reflections at -2000 to -3000 ms, TWT, underlying transparent and low energy reflections, are interpreted as zones of highly strained and sheared material within the crust, i.e., Variscan shear zones and units above as early Carboniferous turbiditic units (*DEKORP Research Group*, 1994b,a; *Fazlikhani et al.*, 2022; *Schäfer et al.*, 2000). Upper Tournaisian-upper Visean turbidites of the Teuschnitz-Ziegenrück Syncline exposed east of the FFS are transected by the seismic profile DEKORP 4N and show transparent and low energy reflections bounded by the high amplitude reflections, partly interpreted as a Variscan shear zone (*DEKORP Research Group*, 1988; *Schäfer et al.*, 2000). A magnetotelluric survey sub-parallel to the seismic profile DEKORP 4N concluded that the high electrical conductivity zone below the Münchberg nappe units is related to the horizontal transport process along the basal shear zones, which is correlated with the observed high amplitude reflections (*Ritter et al.*, 1999). Similar high amplitude reflections in other orogenic settings, e.g. the Scandinavian Caledonides, have also been interpreted as shear zones (e.g., *Fazlikhani et al.*, 2017; *Hurich and Kristoffersen*, 1988; *Juhlin et al.*, 2016).

In the Franconian Platform, intersecting FRANKEN

**Table 3** – Permian and Mesozoic lithologies from wells tied to seismic reflection and gravity model profiles.

| Well | Lithologies from wells tied to gravity models | | | | | | | | |
|---|---|---|---|---|---|---|---|---|---|
| | Quaternary | Jurassic | Keuper | Muschelkalk | Buntsandstein | Zechstein | Rotliegend | Basement | Total depth |
| **Mürsbach 1** | 26 | 0 | 300 | 224 | 524 | 126 | 109 | Not reached | 1309 |
| **Eltmann** | 9.4 | 0 | 178.6 | 235 | 510 | 114 | 3 | 94 | 1144 |
| **Staffelstein 1** | 9 | 102 | 530.2 | 239.8 | 572.2 | 103.8 | 43 | Not reached | 1600 |
| **Staffelstein 2** | 8 | 104 | 532 | 235 | 301 | Not reached | Not reached | Not reached | 1180 |
| **Bad Königshofen** | 3.5 | 0 | 56.5 | 251 | 640 | 76 | Not reached | Not reached | 1027 |
| **Obernsees** | 0 | 140 | 483 | 178.35 | 417.15 | 104.9 | 18.3 | 48.3 | 1390 |
| **Ostheim, Rhön** | 0 | 0 | 0 | 0 | 575 | 217.36 | Not reached | Not reached | 792.36 |

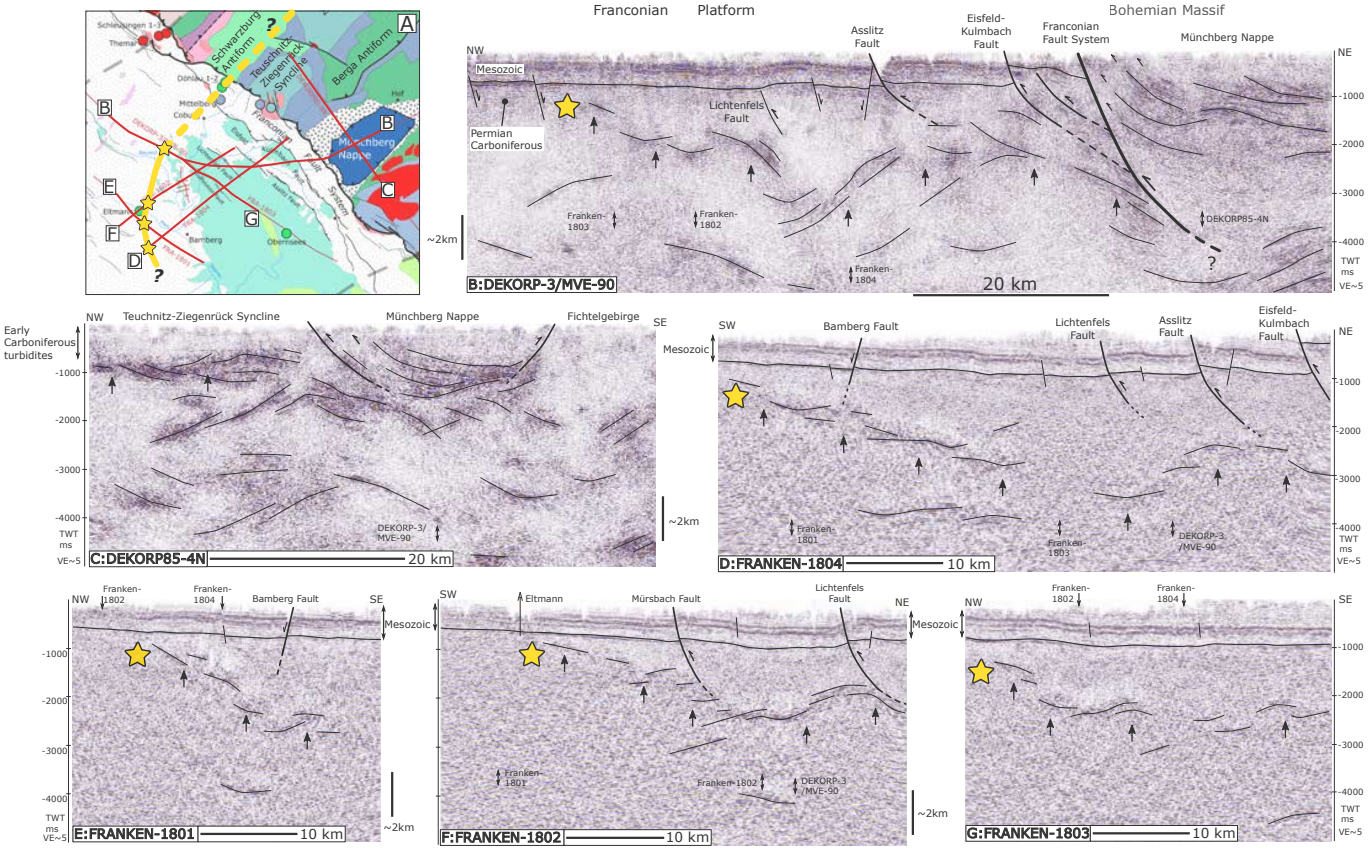


**Figure 3** – 2D Seismic reflection grid imaging the western Bohemian Massif and the Franconian Platform. **(A)** location of seismic reflection profiles, **(B)** DEKORP 3B-MVE90 and (C) DEKORP 4N. **(D-G)** FRANKEN 1801-4 profiles image the subsurface of the Franconian Platform and are tied to the DEKORP 3B-MVE90 profile. High-amplitude and continuous reflections interpreted as Variscan shear zones are overlain by low-amplitude and transparent reflections interpreted as lower Carboniferous turbidites west of the Franconian Fault System (FFS). Yellow stars indicate the west and NW-ward shallowing of the interpreted shear zone in seismic reflection profiles. The yellow line in the inset map shows the map projection of the upper tip of the shear zone covered by younger units.

seismic profiles also image Variscan shear zones below the low energy and semi-transparent reflections that have been interpreted as Palaeozoic metasedimentary rocks and possible Variscan nappe units (*Fazlikhani et al.*, 2022). Interpretation of the intersecting seismic profiles shows the present day geometry and the relationship of possibly different generations of Variscan shear zones (Figure 3). Based on wells and the correlation with the geometry of the lower Carboniferous STB east of the FFS, these low energy and semi-transparent reflections turn out to represent remnants of the lower Carboniferous turbidites bounded by shear zones at depth and covered by Carboniferous-Permian and Mesozoic sedimentary rocks.

High-amplitude reflections, interpreted as Variscan shear zones, generally shallow up toward the west (highlighted by yellow stars on the seismic reflection profiles) reaching to the base/lower parts of the Carboniferous-Permian interval (Figure 3). A projection of the shallowest tip of the shear zones on the map (yellow line in Figures 3A and 4) shows a concave shaped structure dipping mainly to the east and southeast. To the north, where there is a lack of seismic reflection data, the possible extension of the interpreted shear zone is based on the information provided by two wells drilled into basement. Well Mittelberg has encountered the early Carboniferous turbidites while ca. 4 km further north wells Döhlau 1 & 2 are drilled into the older shelf facies (Table 1 and Figure 3A). A possible extension of the mapped shear zone east of the FFS towards the Bohemian Massif is sub-parallel to the boundary between the Teuschnitz-Ziegenrück Syncline and the Schwarzburg Antiform (Figure 4). This boundary is interpreted as the Lehesten Thrust that is developed at 320-310

Ma (latest Variscan NW-SE compressional tectonics) between the Upper Devonian metabasalts and the lower Carboniferous turbidites (*Schäfer et al.*, 2000).

At the SE boundary of the STB close to the Münchberg nappes,a very thick stack (up to 2 s TWT) of variably dipping (apparent dip) high amplitude reflections are interpreted as a mixture of Variscan shear zones, nappe units, deformed lower Carboniferous mass flow deposits and upper shelf facies (*DEKORP Research Group*, 1994a; *Fazlikhani et al.*, 2022; *Franke and Stein*, 2000). Solely based on the seismic reflection data the spatial and temporal relationships between various shear zones and thrusts and highly deformed nappe units at this location cannot be defined, as the entire area is overprinted by NW-directed latest Variscan tectonics and post Variscan deformation (Figure 4).

Pre-Permian Mittelberg and similarly colour coded wells have encountered lower Carboniferous turbidites in the western vicinity of the Teuschnitz-Ziegenrück Syncline, which correlates with the areas of low magnetic field intensity (Figure 5 and Table 1). Further south and southwest, the Eltmann and Obernsees wells did not encounter lower Carboniferous turbidites, instead penetrating into the older Cambrian-upper Tournaisian shelf facies (*Helmkampf*, 2006; *Trusheim*, 1964). The basement rocks in the well Obernsees are recently interpreted as lower Carboniferous turbidites (T. Hahn, Geological Survey of Bavaria, see chapter "model B" for more details). Similarly, basement wells farther SW (Bad Windsheim, Boxberg and Ingelfingen) and south (Boxdorf and wells close the city of Fürth) encountered only Cambrian - upper Tournaisian shelf facies and late-to-post Variscan granites (*Linnemann et al.*, 2010).

## 4.2 Total Magnetic Field Anomaly

Along the Teuschnitz-Ziegenrück Syncline, exposed lower Carboniferous turbidites generally show very low to low magnetic field intensity of -75 to -25 nanoTesla, nT (Figure 5). Very low to low grade metasedimentary rocks of the Cambrian-upper Tournaisian shelf facies on the Berga and Schwarzburg antiforms display low to medium magnetic field intensity of -15 to -45 nT. These rocks locally show very low magnetic field intensity, surrounded by high magnetic field intensity areas (Figure 5). To the NW and north, areas of high magnetic field intensity (>10 nT) represents medium to high-grade gneisses and granitic rocks of the MGCZ, high and ultra-high pressure rocks of the Erzgebirge to the E, and Ordovician and Devonian volcanic rocks (surrounding the Münchberg nappe) to the SE (*Gabriel et al.*, 2011; *Kroner et al.*, 2008; *Linnemann*, 2007; *Schulmann et al.*, 2022). Presented total magnetic field intensity highlights first order and crustal scale structures, the metamorphic and Cadomian basement units as areas with medium to high magnetic field intensity and the metasedimentary and turbidity rocks with low to medium magnetic field intensity in the NW Bohemian Massif. Some of the local highs are related to Variscan intrusions, some of which are exposed at the surface. For instance, the granitic intrusion in the center of the Teuschnitz-Ziegenrück Syncline shows a circular shape and high magnetic field intensity (Figure 5). Very low magnetic field intensity areas (-75 to -25 nT), associated with the upper Tournaisian-upper Visean turbidites along the Teuschnitz-Ziegenrück Syncline, extends SW across the FFS in the area covered by Permian-Mesozoic units of the Franconian Platform (Figure 5). Available pre-Permian wells confirm the presence of the turbidites at the location of very low to low magnetic field intensity areas (Mittelberg, Obernsees, and 6 closely spaced wells shown as two colour coded circles in the vicinity of the FFS, see Table 1 for the list of wells and Figure 5 for the correlation between wells and magnetic field intensity map). It should be mentioned that the shelf facies north and west of the exposed lower Carboniferous turbidites show low but also medium and high magnetic field intensities.

## 4.3 Bouguer Gravity Anomaly

Cambrian - upper Tournaisian metasedimentry rocks and upper-Tournaisian-upper Visean turbidites show intermediate Bouguer gravity values (-20 to 0 mGal, Figure 6). Areas with negative gravity anomalies (≤-20 mGal) mostly correlate with the exposed/drilled late Variscan granites (Figure 6). For instance, negative gravity areas to the NW and SE of the Teuschnitz-Ziegenrück Syncline represent late-to-post orogenic granitic intrusions as confirmed by the exposed granites in the Fichtelgebirge and other places on the Bohemian Massif (in the SW of the Bohemian Massif and exposed/drilled granites in the NW, the Thuringian Hauptgranite, e.g., *Eberts et al.*, 2021; *Thieme et al.*, 2023, Figure 6). Across the FFS to the west, negative gravity anomaly areas are mainly related to assumed granitic intrusions covered by Permian-Mesozoic units of the Franconian Platform (*de Wall et al.*, 2019) and within the MGCZ, Permian (half-)graben and the Mesozoic sedimentary cover. By contrast, positive gravity anomalies ( 0 mGal) are associated to dense crustal units of the MGCZ in the north and NE (Figure 6). Southwest of the study area the NE-SW striking positive gravity anomaly is known as the Kraichgau gravity high that has been interpreted as the Bohemian/Cadomian terrane (*Edel and Weber*, 1995).

## 4.4 Gravity Forward Modelling

We constructed two profiles along the seismic reflection FRANKEN 1802 (Model A, Figure 7) and FRANKEN 1803/DEKORP 3B-MVE90 (Model B, Figure 8) profiles to test the hypothesis on the presence and extent of the lower Carboniferous turbidites to the west of the FFS (see Figure 6 for profiles location). Model A is subparallel to the NE-SW axis of the STB while model B is perpendicular to the basin axis and to model A (Figures 7 and 8). Model A extends NE across the FFS where the lower Carboniferous turbidites are exposed, but this NE portion of model A is beyond the extent of profile FRANKEN 1802 (Figure 7A) and the unit boundaries are based on the surface geology.

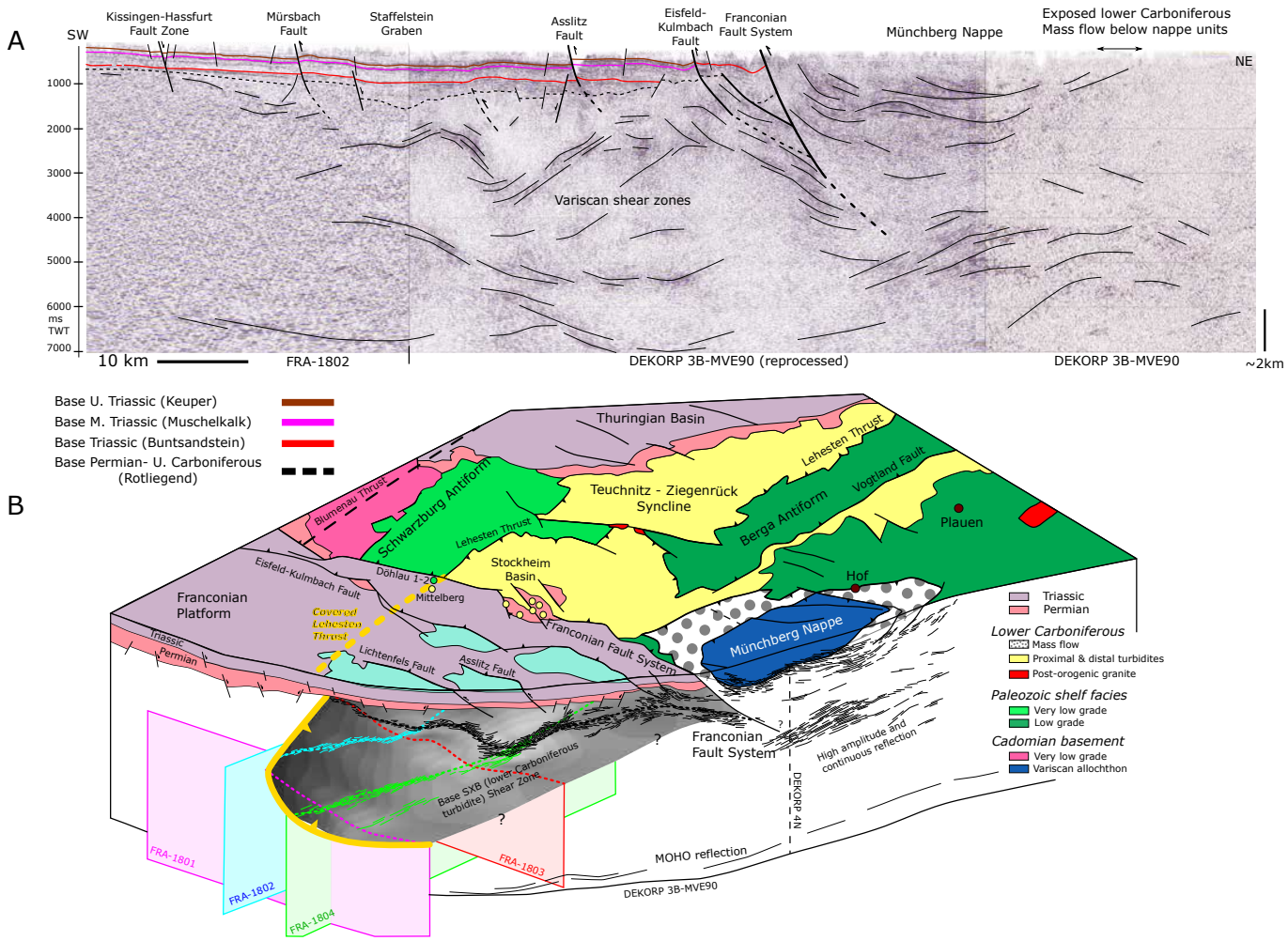


**Figure 4** – 3D geometry of Variscan shear zones in the western Bohemian Massif and the Franconian Platform. (A) The FRANKEN 1802/DEKORP 3B-MVE90 composite profile shows the NE-SW geometry of a Variscan shear zone underlying the lower Carboniferous turbidities and the Münchberg nappe units. (B) Three-dimensional view of the interpreted shear zone (e.g. Lehesten Thrust) covered by Mesozoic units of the Franconian Platform. Colour coded dash lines locate the shear zone (high-amplitude reflections) interpreted from intersecting seismic reflection data. Upper tip of the interpreted shear zone appears to be aligned with the possible SW extension of the Lehesten Thrust beneath the Franconian Platform.

### 4.4.1 Model A: Along the FRANKEN 1802 Profile

The negative gravity anomaly area (-25 to -40 mGal) observed in the center of model A is sub-parallel to the STB axis. The GL-1 gravity low is related to the presence of ca. 3000 m of lower Carboniferous turbidites in the fault block between the FFS and the Eisfeld-Kulmbach Fault (Figure 7). However, parts of the GL-1 is the contribution of ca. 1000 m of Rotliegend, just south of the exposed Rotliegend units in the Stockheim Basin (see Figure 6 for the location of the Stockheim Basin). At this location, the deeper units down to the middle crust have a synform geometry interpreted as a result of up thrusting of Variscan units in the hanging wall of the FFS. A local negative gravity anomaly in the center of the profile in the Staffelstein area represents a Rotliegend half-graben basin, the upper parts of which is drilled by the Staffelstein wells (GL-2 in Figure 7B and C). Towards the SW, the lower Carboniferous turbidites become gradually thinner to zero at the Eltmann well site, where below the ca. 3 m of Rotliegend units, Devonian metasediments (shelf facies) are drilled (*Trusheim*, 1964). In the SW parts of Model A, a sub-parallel and elongated gravity low is interpreted as the out-of-plane influence of a nearby modeled granitic intrusion (Hassfurt granite in Figure 6, GL-3 in Figure 7; see also *de Wall et al.*, 2019). If only excluding the influence of the Hassfurt granite the model show an RMS error of 3.1, about 5 times higher than the best fit model which has an RMS error of 0.63 (Figure 7B, violet line shows the model excluding Hassfurt granite, and the red line is the best fitting model). Inner shelf facies (Cambrian-lower Carboniferous metasediments) in the footwall of the FFS are gently folded, accounting for the observed regional-scale gravity anomaly, whereas local gravity anomalies are attributed to shallower and localized rock bodies. For example, the regional gravity high (GH-1) in the NE edge of Model A is related to the combined effects of the Devonian diabase exposed in the S-SW parts of the Berga Antiform and the uplift of the deeper basement units in the hanging wall of the FFS (Figure 7). The best fitting model was obtained by including the lower Carboniferous turbidites below the Permian-Mesozoic units (red line in Figure 7B). Our modelling result indicates that scenarios assuming

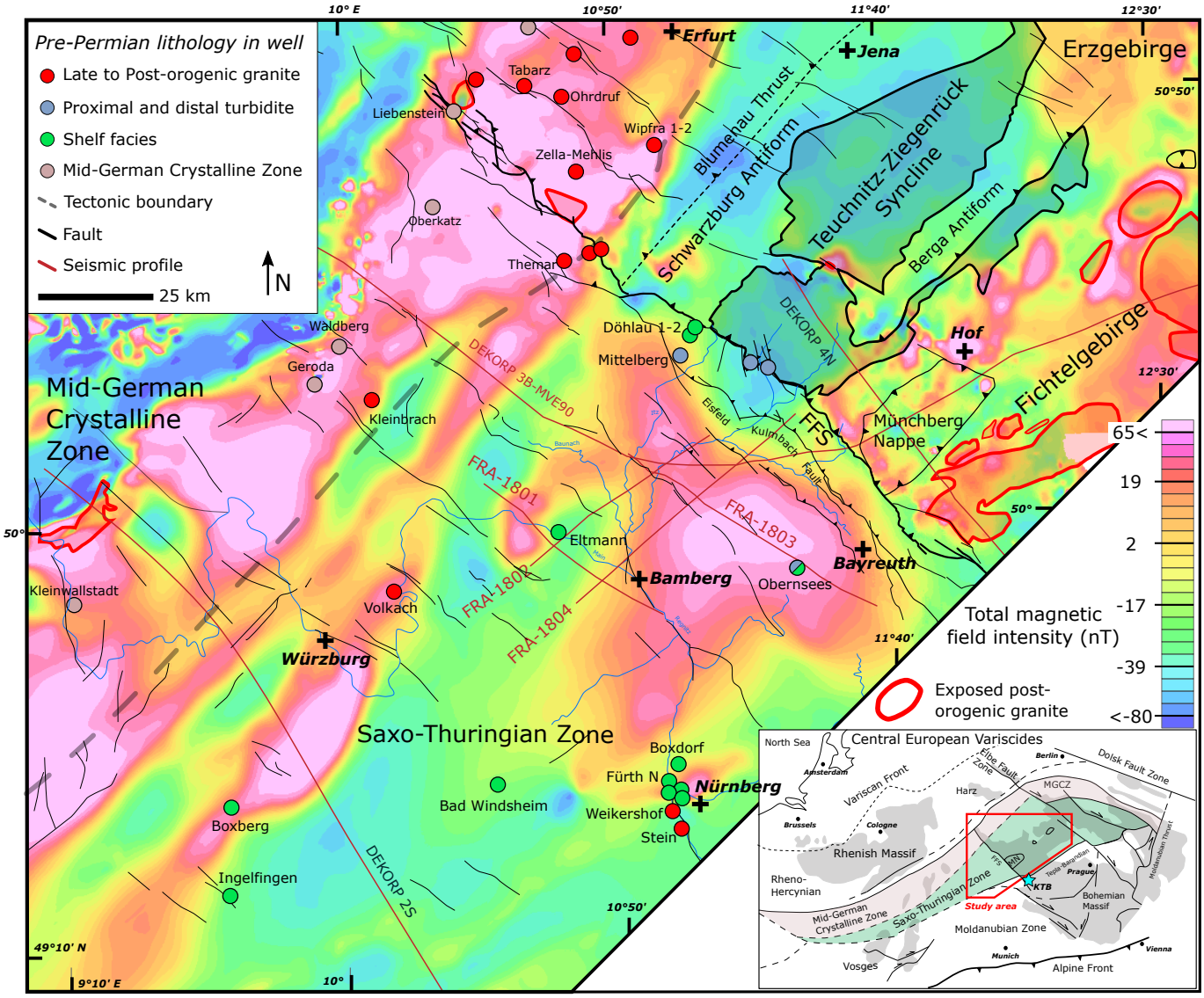


**Figure 5** – Total magnetic intensity map of the study area illustrating a general NE-SW orientation of Variscan units (Gabriel et al., 2011). The Teuschnitz-Ziegenrück Syncline in the West Bohemian Massif shows low magnetic field intensity (-30 to -75 nT). Across the Franconian Fault System (FFS) this low magnetic field intensity area extends SW-ward and is drilled by 7 wells (see Table 1).

only Permian rocks (green line in Figure 7B) or only shelf facies (blue line in Figure 7B) instead of the lower Carboniferous turbidites below the Mesozoic cover lead to larger RMS errors of 3 to 4 orders of magnitude.

### 4.4.2 Model B: Along the Composite FRANKEN 1803/DEKORP 3B-MVE90 Profile

Perpendicular to the STB axis, Model B shows the NW and the SE extension of the basin (Figure 8). In the NW the Mid German Crystalline Zone (MGCZ) shows transparent reflectivity and a regional gravity low belt that is related to the granitic intrusions exposed and drilled along the MGCZ (Figure 8A and B). High amplitude and dipping reflections SE of the MGCZ have been interpreted as the Vesser magmatic arc (Vesser Zone) and the suture zone between the STZ in the SE and the MGCZ to the NW (*DEKORP Research Group*, 1994a; *Schäfer et al.*, 2000). This area shows a high gravity anomaly and is modeled with folding and thrusting of basement units, also described as the Northwest-Wrench and Thrust Zone (NW-WTZ, *Kroner et al.*, 2007, Figure 8B and C). Local gravity lows along this regional gravity high are related to the Permian graben and half-graben structures (Figure 8B and C). The negative gravity anomaly in the SE of the profile is attributed to the lower Carboniferous turbidites and to a lesser extent to the thicker remaining Mesozoic units (GL-1, Figure 8B and C). Similar to Model A, scenarios with only Permian (green line) or shelf facies (blue line) below the Permian units cause higher RMS errors (Figure 8B). The best fitting model with lower Carboniferous turbidites is shown in Figure 8C which corresponds to the red line in Figure 8B. In the SE extremity of the profile observed GL-2 gravity low is related to a Permian graben and a possible granitic intrusion in the middle crust (Bayreuth granite, *de Wall et al.*, 2019). At this location, the Obernsees well is located 1000 m SW of the profile and drilled into the basement rocks that were originally interpreted as

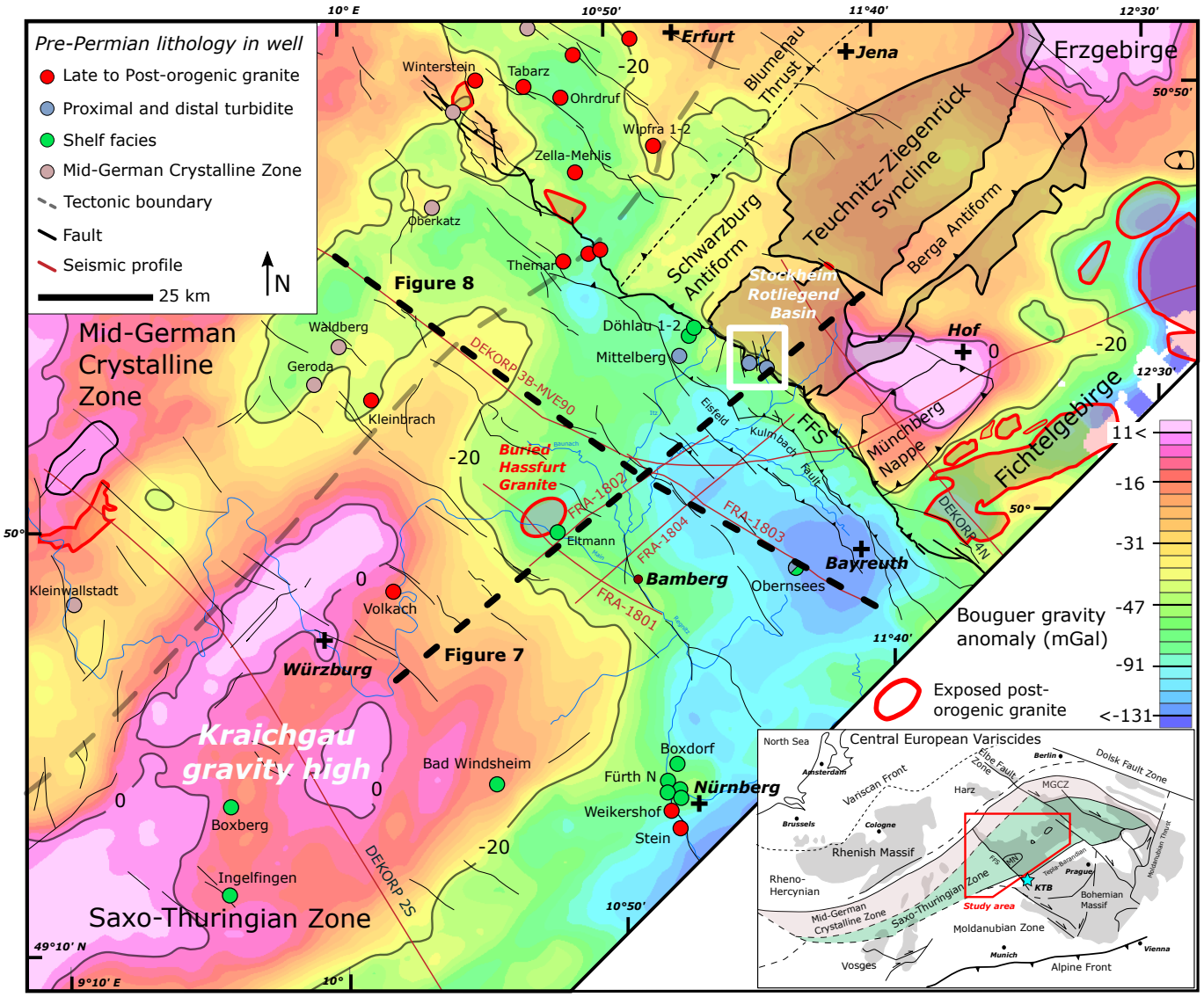


**Figure 6** – Bouguer gravity anomaly map of the study area and basement wells. Lower Carboniferous turbidites tend to correlate with a medium gravity anomaly while the Variscan granites (red polygon) are characterized by a negative Bouguer gravity signature. Elevated gravity values (>-20 mGal) in the SE reflect the Kraichgau gravity high, which is bounded to the NW by a regional gravity low. The regional negative gravity belt has been shown to be an area of granitic intrusion as indicated by several wells and exposed granites known as "Thuringian Hauptgranite". Modelled Hassfurt granite is shown in the center of the study area

the shelf facies (Devonian metasediments, *Stettner and Salger*, 1985, the models presented in Figure 8B and C are based on this interpretation). However, recently the basement rocks in well Obernsees are re-interpreted as the lower Carboniferous turbidites (see Appendix B in Supporting Information) and models shown in Figure 8D and E are based on this new interpretation of the basement rocks. The assumption of lower Carboniferous turbidites in the SE part of the profile implies that the STB extends further to the SE, most likely close to the Saxo-Thuringian-Moldanubian boundary. Green and blue lines in Figure 8D show models where lower Carboniferous turbidites are replaced by the Permian or shelf facies, respectively, causing higher RMS errors.

# 5 Discussion

## 5.1 Saxo-Thuringian Basin Extent West of the Bohemian Massif

Lithologies encountered by the basement wells and low magnetic field intensity areas west of the FFS suggest that the lower Carboniferous turbidites extend ca. 20 km SW from the exposed turbidites in the NW Bohemian Massif. On the other hand, seismic reflection interpretation and forward gravity models suggest that the lower Carboniferous turbidites occupy larger areas and possibly extend ca. 60 km SW. The latter is supported by drilled Palaeozoic shelf facies overlaid by the Carboniferous-Permian units in the Eltmann well (Figures 4 and 5).

To the NW, well Mittelberg encounters lower Carboniferous turbidites while further 4 km north, wells Döhlau 1 and 2 encounter Devonian and older rocks,

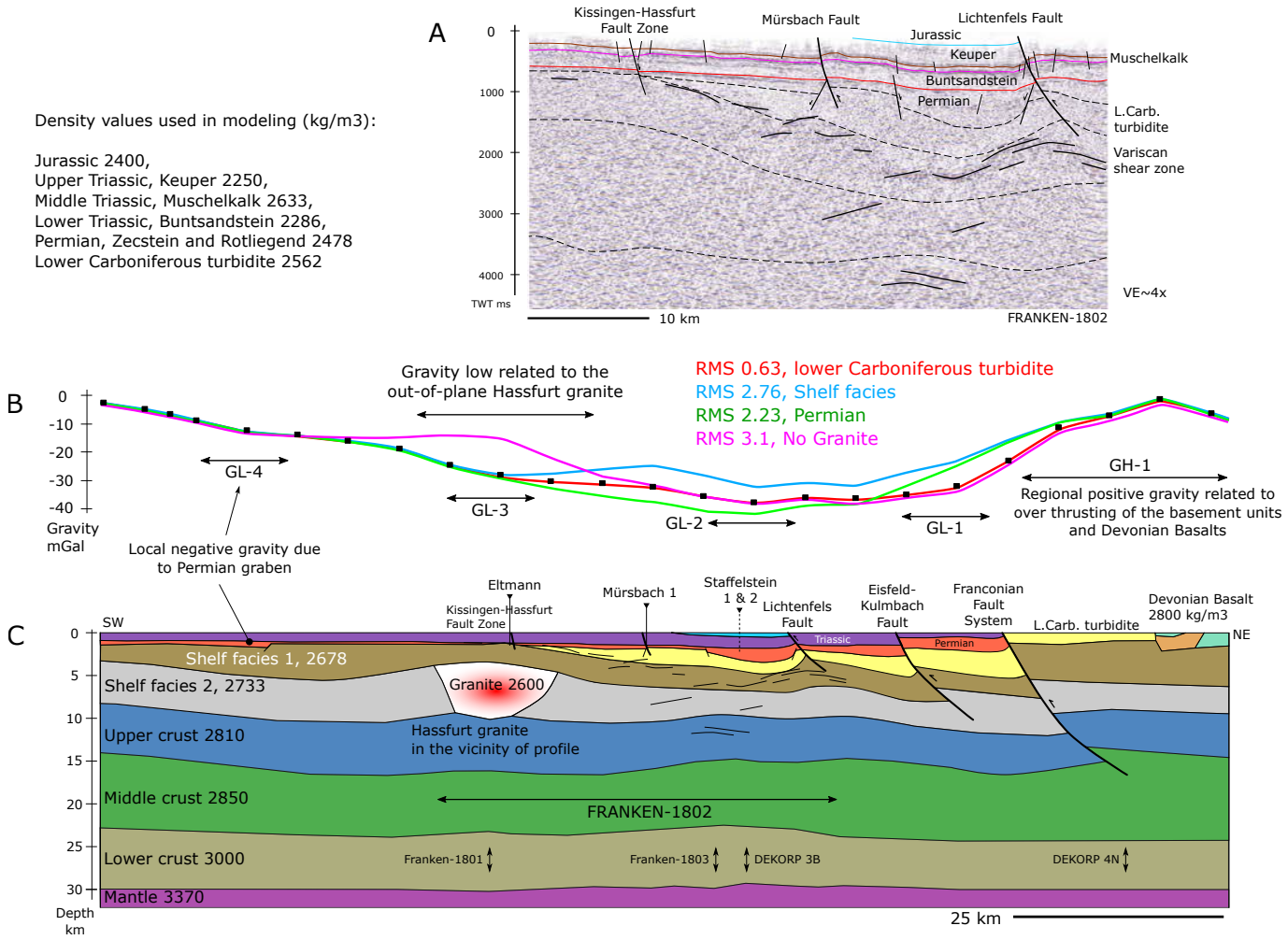


**Figure 7** – Forward gravity model along the FRANKEN 1802 seismic profile. Mesozoic and top of Permian horizons are based on the seismic interpretation tied to wells (see Table 3 for the Permian and Mesozoic lithologies from wells). Panel A is the interpretation of the seismic profile FRANKEN 1802 showing the geometry of Permian and Mesozoic horizons, Variscan shear zone and middle crustal units. Panel B shows the measured gravity anomaly (dotted line) and four scenarios modeled with corresponding Root-Mean-Square (RMS) errors. The best fitting model is achieved by incorporating lower Carboniferous turbidites (red line). Assuming only Permian (green line) or only shelf facies (blue line) instead of lower Carboniferous turbidites, models show higher RMS errors. The violet line shows the scenario when excluding the Hassfurt granite effect located in the vicinity of the profile. Panel C illustrates the final model with lower Carboniferous turbidites (red line in panel B) and the out-of-plane influence of the Hassfurt granite. The regional gravity high (GH-1) in the NE of the profile is due to the uplift of deeper and denser basement rocks and Devonian basalts in the hanging wall of the FFS. Local negative gravity anomalies (GL-1 to 4) are mainly related to the Permian grabens.

suggesting the NW limit of the STB. This observation supports the interpretation of the Variscan shear zone in seismic reflection data to be developed between lower Carboniferous turbidites and the older shelf facies. However, the magnetic field intensity map shows similar signatures at the location of the Döhlau and Mittelberg wells, which can be due to the low magnetization of the Palaeozoic metasedimentary units (Figure 5).

Based on outcrop analysis and K-Ar dating, *Schäfer et al.* (2000) conclude that in the NW parts of the STZ the deformation occurred after 320 Ma and terminated at ca. 310 Ma. This is the time interval at which the Lehesten Thrust is developed during the latest Variscan NW-SE compressional tectonics between the Upper Devonian metabasalts and the lower Carboniferous turbidites (*Schäfer et al.*, 2000). However, the arcuate geometry and westward shallowing of the interpreted shear zone suggest that it might have been developed as a strike-slip shear zone related to a top-to-the SW tectonic transport prior and coeval to sedimentation of the upper Tournaisian-upper Visean turbidites. This strike-slip shear zone was potentially reactivated during the latest Variscan tectonics in a top-to-the SE tectonic transport as a thrust shear zone (*Stephan et al.*, 2016), locally overprinting its initial SW-directed development. Detailed mapping and analysis of *Hahn et al.* (2010) show that the distal turbidite sedimentation started at ca. 342 Ma, before the deformation has started in the NW of the STZ and hence the NW parts of the STB. Therefore, the lower Carboniferous turbidity basin is not controlled by or developed on top of a shear zone (here the Lehesten Thrust/shear zone) similar to the classical piggy-back basin in the orogenic belts (*Busby and Ingersoll*, 1995). To the SE, defining the basin boundary is more challenging owing to the lack of the seismic

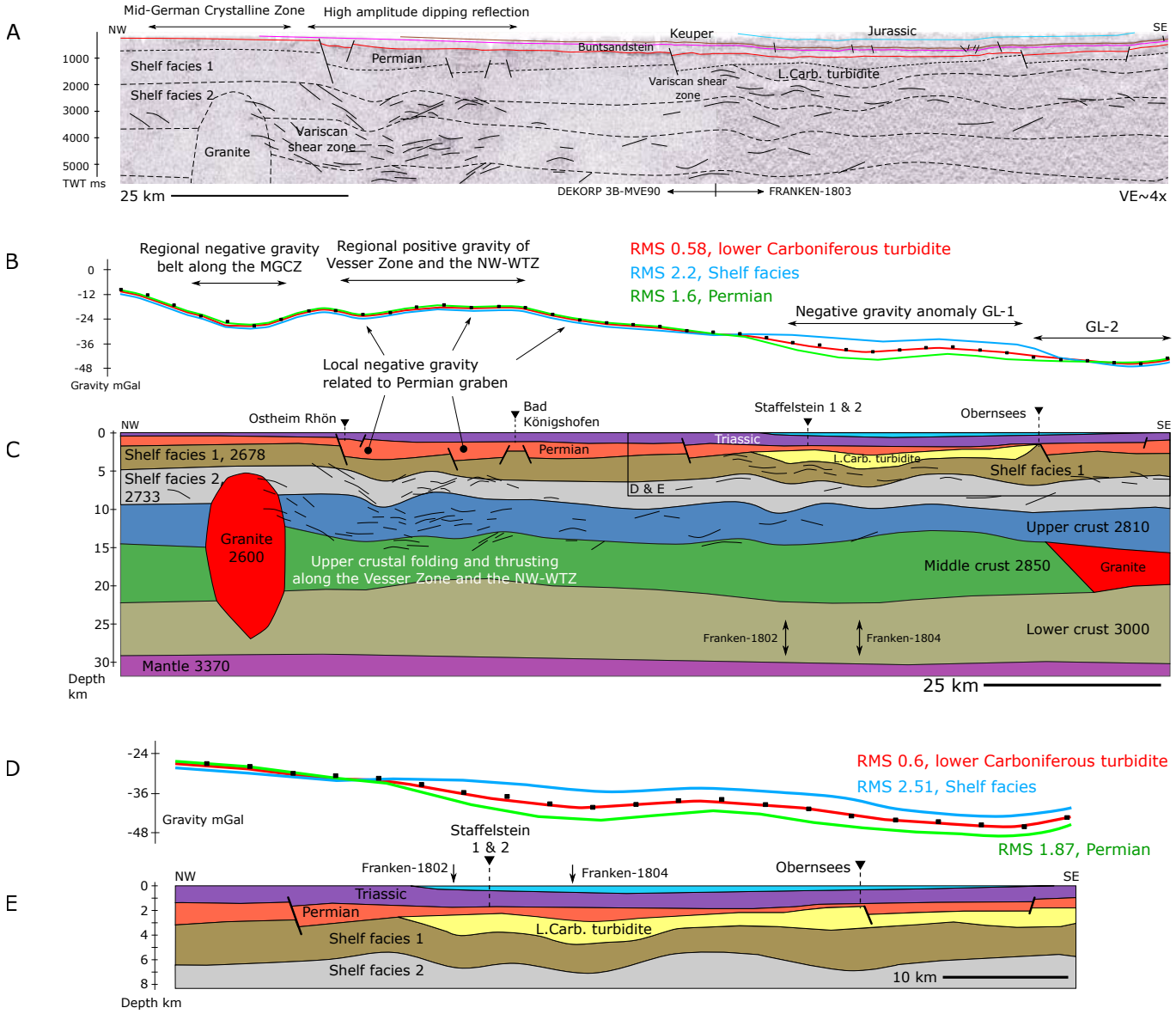


**Figure 8** – Forward gravity model along the composite FRANKEN 1803/DEKORP 3B-MVE90 profile. See Figure 7 for the density values used in the modelling and Table 3 for the Permian and Mesozoic lithologies from wells. Panel A is a composite FRANKEN 1803/DEKORP 3B-MVE90 profile showing stratigraphical units, major Permian basins, Variscan shear zones and related folding. Panel B illustrates measured gravity anomaly (dotted line) and three scenarios modeled with corresponding Root-Mean-Square (RMS) errors. The best fitting-model is achieved by incorporating lower Carboniferous turbidites (red line). Models assuming only Permian (green line) or only shelf facies (blue line) instead of lower Carboniferous turbidites show higher RMS errors. Panel C shows the final model with lower Carboniferous turbidites (red line in panel B). The regional negative gravity anomaly in the NW (panel B and C) is modeled by granitic intrusion along the Mid German Crystalline Zone (MGCZ) while the adjacent gravity high is related to the upper crustal folding and thrusting along the Vesser Zone and the Northwest Wrench and Thrust Zone (NW-WTZ). Panel B and C are models based on the original interpretation of the basement rocks in well Obernsees as the "shelf facies". Note that the well Obernsees is located 1000 m SW of the profile in the footwall of a Permian graben. Panel D shows models based on the recent interpretation of the basement rocks in well Obernsees as "lower Carboniferous turbidite". Similarly, scenarios at which there is only shelf facies (blue line) or Permian units (green line) below the Mesozoic cover are modeled. Panel E shows the final model with lower Carboniferous turbidites below the Permian graben (red line in panel D).

reflection and well data. The SE boundary of the basin on the Bohemian Massif is also unclear (*Falk et al.*, 1995; *Hahn et al.*, 2010). Basement rocks being drilled by the well Obernsees have originally interpreted as Palaeozoic shelf facies based on the assumption that the reddish colour of the units is of a primary nature even if there are evidences showing a secondary nature of the reddish colour (*Helmkampf*, 2006; *Stettner and Salger*, 1985). According to this interpretation the lower Carboniferous turbidites are absent at well Obernsees. However, by a recent interpretation based on the lithostratigraphic correlation with exposed Palaeozoic shelf facies and the secondary nature of the observed reddish colour, the basement rocks in the well Obernsees are assigned to the lower Carboniferous turbidities (Leutenberg Group, Bavarian Environment Agency (LfU), see Appendix B in Supporting Information). With the shelf facies as the basement rocks, the model requires 1400 m of Permian

units, which is not supported by the observed seismic facies, while with the presence of the lower Carboniferous turbidites, the model is satisfied with 800 m of Permian rocks (Figure 8C and E).

## 5.2 The Saxo-Thuringian Basin a 'Lateral Foreland' Basin

The STB has been previously studied based on the outcrop observations and used to explain the NW-SE collisional tectonic scenario (*Franke*, 1984b). In such a view, deposition in a long lived Palaeozoic marine basin changed to synorogenic deep marine sedimentation due to flexural loading in the southeast. Ongoing northwest directed nappe transport transformed such a flexural foreland basin in a late Variscan subcylindrical fold- and thrust-belt. As mentioned above, this traditional view is in conflict with various constraints as it cannot explain the complex and prolonged tectono-metamorphic record in the allochthonous units of the STZ (*Jouvent et al.*, 2022; *Schulz and Krause*, 2024). Moreover, the axis of the STB is parallel to the initial NE-SW nappe transport, and on the southeastern margin of the basin the mass flows were deposited on already exhumed metasediments (*Hahn et al.*, 2010). Therefore, the STB cannot be explained as a flexural foreland basin caused by prolonged and exclusive NW-SE convergence. The SW extent of the STB described here, appears to be less affected by the NW-SE oriented Variscan tectonics as it is positioned in the low-strain area between the transform plate boundary and the lateral edge of the collisional pile (high-strain areas, Figure 9 cross-sections X-X', and Y-Y'). Late Variscan NNW-SSE compression is highly oblique compared with the NE-SW oriented Gondwana-Laurussia plate convergence and postdates the sedimentation of the STB (*Kroner and Romer*, 2010).

The STB evolved adjacent to the Gondwana-Laurussia plate boundary that is represented by the NE-SW oriented MGCZ (Figure 9). This sinistral lithospheric-scale shear zone strikes parallel to the small circle trajectories of the Gondwana-Laurussia Euler pole (*Kroner et al.*, 2016, 2022), representing a transform fault connecting the convergent plate boundary of the French Massif Central with the frontal collision zone at the NE edge of the Bohemian Massif (*Stephan et al.*, 2016). Thus, the syncollisional STB evolved in a marginal position and low-strain zone between a transform plate boundary in the NW and the lateral edge of the collisional pile of the Bohemian Massif in the SE (Figure 9). As evidenced by the NE-SW arranged proximal synorogenic deposits NW of the Fichtelgebirge, this voluminous collisional pile constitutes the boundary of the STB in the SE. Because the transform plate boundary in the NW (future MGCZ and the NW-WTZ) did not significantly contribute to the basin infill, the STB was exclusively supplied by detritus from the collisional pile (equivalent of the Erzgebirge-Fichtelgebirge Zone) in the SE. Nevertheless, in some respect the depositional environment is similar to classical foreland basins. For example, the southeastern boundary of the STB is adjacent to the thickened collision zone, and the uplifting collisional wedge delivered detritus to the basin. Moreover, the transition from distal to proximal sediments changed through time from SE to NW.

There are differences between the STB and classical foreland basins. The sedimentation occurred in a strike-slip dominated part of the plate boundary zone, and the basin boundaries are characterized by strike-slip faulting. One of these faults constitutes the boundary fault to the collisional wedge. No initial flexural bending occurs and the axis of this narrow basin is parallel or acute-angled to the convergence direction during the collision. Late orogenic deformation after the overfill stage is able to obliterate the initial architecture of the basin. To distinguish such an architecture from classical foreland basins, we propose the term "lateral foreland basin".

## 5.3 Implication for the Variscan Tectonics

Radial transport directions of lower Carboniferous tubidites from surrounding highlands into the spoon shaped STB, suggest that the northwest and west parts of the STZ also sourced sediments into the basin. However, at the latest stages of the basin fill (at the time of deposition of the proximal turbidite) sedimentary input from the northwest and west increases before the STB becomes over-filled (*Franke*, 1984a; *Gräbe and Wucher*, 1967; *Hahn et al.*, 2010). Contrasting to this observation is that so far no sign of sediments sourced from the MGCZ in the NW of the STB has been detected (*Eder et al.*, 1983; *Falk et al.*, 1995). Based on the architecture of the STB, occupying low-strain areas of the STZ, source of sediments and transport direction discussed above, we propose that the northwest and west areas of the STB, i.e. the high-strain zone (future MGCZ and the NW-WTZ) experienced transpression and uplift during lower Carboniferous time coeval to the ongoing sedimentation in the STB. Deformation and uplift of the high-strain zone continues during the Carboniferous producing detritus feeding the STB and eventually exposes the crystalline basement. At the time of which the crystalline basement is exposed in the NW, the STB is already over-filled and therefore erosional products are transported north-ward into the Rheno-Hercynian basin (Figure 9B and cross section X). Our interpretation can explain described radial transport directions into the STB and at the same time the lack of detritus sourced from the MGCZ in the NW, and it is supported by the U-Pb ages obtained from detrital and magmatic zircons farther north (*Linnemann et al.*, 2024). Spatial deformation of the STZ and surrounding high-strain areas are also heterogeneous. While the SE and the central low-strain parts of the STZ accommodated distal turbidites, the remaining part of the STZ was still in a marine environment. The general pattern of coarser grained and more proximal facies in the SE versus more distal facies towards the NW of the basin is the common configuration of the STB. Such heterogeneous temporal and spatial deformation and sedimentation explains the coexistence of the high and low strain (partly occupied by the STB) areas in the

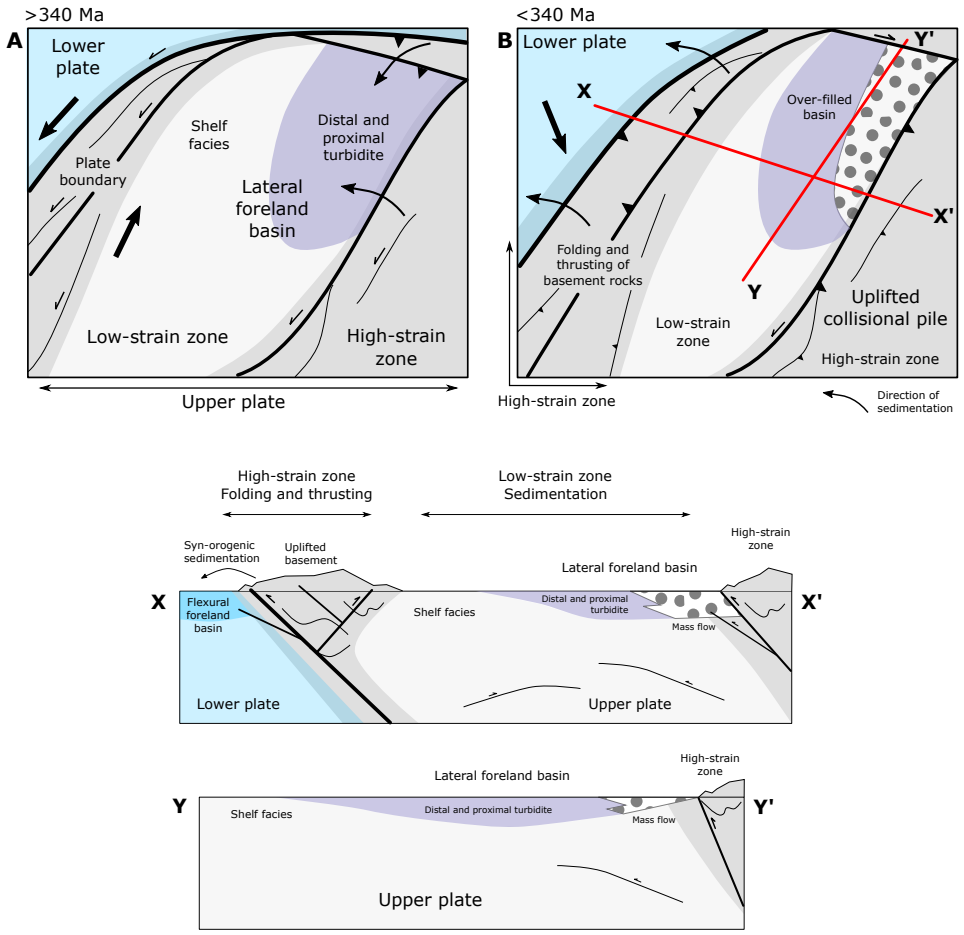


**Figure 9** – Simplified sketch showing the position of the "lateral foreland" basin on the upper plate. The lateral foreland basin is bordered by a collisional pile on one side and the transform plate boundary on the other side. **A)** shows the STB development in the low-strain areas accommodating detritus sourced from the NE and the SE while the NW areas still in a marine environment. **B)** illustrates the over-filled stage of the basin and the NW-ward over-thrusting of the collisional pile and uplifting of basement rocks in the high-strain area in the NW (i.e. MGCZ in the study area). At this stage the NW high-strain area is the major sedimentary source area towards the NW, into the northern foreland basin (i.e. the Rheno-Hercynian basin) while to the SE the lateral foreland basin is already overfilled. Cross-sections X-X' and Y-Y' show across and along basin geometry and underlying units, respectively.

STZ between the Laurussia-Gondwana transform plate boundary and the lateral edge of the Variscan collisional pile.

## 5.4 An integrated Methodology for Subsurface Characterization

Information about the subsurface rock types in the study area, such as Permian clastics (Rotliegend), lower Carboniferous turbidites, Palaeozoic shelf facies or orogenic granitic intrusions, influence subsurface development strategies. For instance, identified lower Carboniferous turbidites and Permian fault-bounded basins (graben and half-graben structures) above the possible granitic intrusions can be investigated as potential reservoirs in the course of deep geothermal investigations, despite having medium to low porosities (*Drews et al.*, 2019; *de Wall et al.*, 2019). Equally important is the characterization of the subsurface structural discontinuities and their spatial evolution bounding the reservoir rocks, here Permian and Mesozoic units. Some of the Permian deep-reaching normal faults are blind, while some others localize strain and got reactivated as reverse faults during Mesozoic tectonic activities (*Fazlikhani et al.*, 2022; *Köhler et al.*, 2022; *Wiest et al.*, 2025). Such multiphase activity and deep reaching Permian faulting increase structural permeability, and thus fluid transport capacity in tight granitic reservoirs in the case of enhanced geothermal systems. The presence and extent of the Variscan granitic intrusion modeled in the study area has also been discussed previously (*de Wall et al.*, 2019), the presented approach however, better constrains the subsurface rock units and structural patterns as important parameters for estimating the deep geothermal potential in the study area. The integrated methodology presented here can be applied as a first step to characterize the subsurface, especially in the underexplored regions or areas with very limited subsurface data, in response to the growing need to diversify energy resources (e.g. deep geothermal and natural hydrogen) and to understand the subsurface geological settings in estimating storage capacities (e.g. $CO_2$, $H_2$ or nuclear waste).

## 6 Conclusion

In this study, we integrate magnetic, gravity, seismic reflection and well data to characterize the subsurface lithologies and structures in the western Bohemian Massif, central European Variscides. The results of our interpretation and modelling demonstrate that:

1. The lower Carboniferous turbidites exposed in the NW Bohemian Massif, extend approximately 60 km west of the Franconian Fault System. These units exhibit low energy and transparent reflections in both exposed (NW Bohemian Massif) and covered (Franconian Platform) portions of the basin. The lower Carboniferous turbidites are separated from Devonian and older rocks by high amplitude and continuous reflections interpreted as Variscan shear zones.
2. Based on our modelling results and published field studies, we define the Saxo-Thuringian Basin as a "lateral foreland" basin because it is located in the upper plate in a marginal position relative to the collisional pile. The STB evolved in a low-strain zone between two high-strain zones, the transform plate boundary in the NW (future Mid German Crystalline Zone) and the lateral edge of the collisional pile of the Bohemian Massif.
3. Gravity highs in the Franconian Platform are related to the folding and thrusting of the basement rocks while the gravity lows are likely related to the late- to post-orogenic granitic intrusions and local Permian graben and half-graben structures.

## Acknowledgements

We would like to thank the Bayerisches Landesamt für Umwelt (LfU) for providing well data and Torsten Hahn for fruitful discussions regarding the basement rocks in the Obernsees well. Schlumberger is thanked for providing academic licenses for Petrel and supporting the "3D Lab" at the Friedrich–Alexander University (FAU) Erlangen–Nürnberg. LIAG Institute for Applied Geophysics and Prof. Gerald Gabriel are thanked for providing the Bouguer gravity anomaly and the total magnetic intensity grids, as well as the GFZ German Research Center for Geosciences and Dr. Manfered Stiller for handling and sharing the DEKORP seismic reflections profiles. Authors would also like to thank Stanislaw Mazur and two unknown reviewers for their comments on an earlier version of the paper. This contribution is part of the Geothermal Alliance Bavaria (GAB) project, which is funded by grants from the Bavarian State Ministry of Education and Cultural Affairs, Science and Art provided to the Friedrich–Alexander University (FAU) Erlangen–Nürnberg and partners.

## Author contributions

**Hamed Fazlikhani:** conceptualization, investigation, methodology, funding and geophysical data acquisition team, writing – original draft. **Uwe Kroner:** conceptualization, writing – review and editing. **Harald Stollhofen**, **Wolfgang Bauer** and **Daniel Koehn:** writing-review and editing, funding and geophysical data acquisition team.

## Data availability

Bouguer gravity anomaly and total magnetic field intensity grids are available from the LIAG Institute for Applied Geophysics. Original DEKORP seismic reflection survey is available from the GFZ (Deutsches GeoForschungsZentrum) Potsdam upon request. Well data are available through the Geological Survey of Bavaria (Bayerisches Landesamt für Umwelt – LfU). FRANKEN seismic data are acquired for the ongoing Geothermal Alliance Bavaria (GAB) research project and are not yet publicly available.

## Competing interests

The authors declare no competing interests.

## Peer review

This publication was peer-reviewed by Wolfram Geissler and an anonymous reviewer. The full peer-review report can be found here: Review Report.

## Copyright notice



## References

Andreas, D. (2013), Der Thüringer Wald im Zeitraum der Stefan-Unterperm-Entwicklung - ein Abschnitt der Zentraleuropäischen N-S-Riftzone innerhalb des Mitteleuropäischen Großschollenscharniers, Ph.D. thesis, Technical University of Freiberg, Freiberg, Germany.

Andreas, D., H. Haubold, and G. Katzung (1975), ZUR GRENZE STEFAN/AUTUN (KARBON/PERM), *Zeitschrift für Geologische Wissenschaften*, *3*(6), 699 A 716.

Anthes, G., and T. Reischmann (2001), Timing of granitoid magmatism in the eastern mid-German crystalline rise, *Journal of geodynamics*, *31*(2), 119–143, doi: http://doi.org/10.1016/s0264-3707(00)00024-7.

Bosum, W., U. Casten, F. C. Fieberg, I. Heyde, and H. C. Soffel (1997), Three-dimensional interpretation of the KTB gravity and magnetic anomalies, *Journal of geophysical research*, *102*(B8), 18,307–18,321, doi: http://doi.org/10.1029/96jb03407.

Brosin, P., and H. Lützner (2012), Verdeckte Rotliegend-Vorkommen zwischen Thüringer Wald und

Harz, *Schriftenreihe der Deutschen Gesellschaft für Geowissenschaften*, pp. 488–503.

Busby, C., and R. Ingersoll (1995), Tectonics of sedimentary basins, *Oxford, Blackwell Science*.

De Wall, H., and H. Stollhofen (2016), *Erkundung des geologischen Untergrundes in Nordost-Bayern als Grundlage zur Bewertung des geothermischen Potenzials. Abschlussbericht März 2016, GeoZentrum Nordbayern*, Erlangen.

De Wall, H., and H. Stollhofen (2017), *Erkundung des geologischen Untergrundes in Nordost-Bayern als Grundlage zur Bewertung des geothermischen Potenzials. Abschlussbericht der Projektverlängerung (3. Jahr), GeoZentrum Nordbayern*, Erlangen.

de Wall, H., A. Schaarschmidt, M. Kämmlein, G. Gabriel, M. Bestmann, and L. Scharfenberg (2019), Subsurface granites in the Franconian Basin as the source of enhanced geothermal gradients: a key study from gravity and thermal modeling of the Bayreuth Granite, *International journal of earth sciences*, *108*(6), 1913–1936, doi: http://doi.org/10.1007/s00531-019-01740-8.

DEKORP Research Group (1988), Results of the DEKORP 4/KTB Oberpfalz deep seismic reflection investigations, *Journal of Geophysics*, *62*, 69–101.

DEKORP Research Group (1994a), Crustal structure of the Saxothuringian Zone: Results of the deep seismic profile MVE-90(East), *Zeitschrift für Geologische Wissenschaften*, *22*(6), 647–769.

DEKORP Research Group (1994b), DEKORP 3/MVE 90(West) - preliminary geological interpretation of a deep near-vertical reflection profile between the Rhenish and Bohemian Massifs, Germany, *Zeitschrift für Geologische Wissenschaften*, *22*(6), 771–801.

Drews, M., W. Bauer, H. Fazlikhani, H. Stollhofen, M. Kämmlein, M. Potten, K. Thuro, and H. de Wall (2019), Ursachenforschung zur geothermischen Anomalie in Nordbayern, *Geothermische Energie*, *91*, 10–13.

Eberts, A., H. Fazlikhani, W. Bauer, H. Stollhofen, H. de Wall, and G. Gabriel (2021), Late to post-Variscan basement segmentation and differential exhumation along the SW Bohemian Massif, central Europe, *Solid earth*, *12*(10), 2277–2301, doi: http://doi.org/10.5194/se-12-2277-2021.

Eckhardt, F. J. (1962), Über einen Natronsyenit im kristallinen Untergrund Unterfrankens, *Neues Jahrbuch für Mineralogie, Monatshefte*, *1962*, 109–114.

Edel, J. B., and K. Weber (1995), Cadomian terranes, wrench faulting and thrusting in the central Europe Variscides: geophysical and geological evidence, *Geologische Rundschau*, *84*(2), 412–432, doi: http://doi.org/10.1007/bf00260450.

Eder, F. W., W. Engel, W. Franke, and P. M. Sadler (1983), Devonian and carboniferous limestone-turbidites of the rheinisches schiefergebirge and their tectonic significance, in *Intracontinental Fold Belts*, edited by H. Martin and F. W. Eder, pp. 93–124, Springer Berlin Heidelberg, Berlin, Heidelberg, doi: http://doi.org/10.1007/978-3-642-69124-9_5.

Enderle, U., K. Schuster, C. Prodehl, A. Schulze, and J. Bribach (1998), The refraction seismic experiment GRANU95 in the Saxothuringian belt, southeastern Germany, *Geophysical journal international*, *133*(2), 245–259, doi: http://doi.org/10.1046/j.1365-246X.1998.00462.x.

Falk, F., W. Franke, and M. Kurze (1995), Stratigraphy, in *Pre-Permian Geology of Central and Eastern Europe*, edited by R. D. Dallmeyer, W. Franke, and K. Weber, pp. 221–234, Springer Berlin Heidelberg, Berlin, Heidelberg, doi: http://doi.org/10.1007/978-3-642-77518-5_23.

Fazlikhani, H., H. Fossen, R. L. Gawthorpe, J. I. Faleide, and R. E. Bell (2017), Basement structure and its influence on the structural configuration of the northern North Sea rift, *Tectonics*, *36*(6), 1151–1177, doi: http://doi.org/10.1002/2017TC004514.

Fazlikhani, H., W. Bauer, and H. Stollhofen (2022), Variscan structures and their control on latest to post-Variscan basin architecture: insights from the westernmost Bohemian Massif and southeastern Germany, *Solid earth*, *13*(2), 393–416, doi: http://doi.org/10.5194/se-13-393-2022.

Franke, W. (1984a), *Variszischer Deckenbau im Raume der Münchberger Gneismasse - abgeleitet aus der Fazies, Deformation und Metamorphose im umgebenden Paläozoikum*, Geotektonische Forschungen, Schweizerbart'sche, E, Stuttgart, Germany.

Franke, W. (1984b), Late events in the tectonic history of the Saxothuringian zone, *Geological Society special publication*, *14*(1), 33–45, doi: http://doi.org/10.1144/gsl.sp.1984.014.01.04.

Franke, W. (1989), Tectonostratigraphic units in the Variscan belt of central Europe, in *Terranes in the Circum-Atlantic Paleozoic Orogens*, *Geological Society of America Special Papers*, vol. 230, edited by R. D. Dallmeyer, pp. 67–90, Geological Society of America, doi: http://doi.org/10.1130/spe230-p67.

Franke, W., and E. Stein (2000), Exhumation of high-grade rocks in the Saxo-Thuringian Belt: geological constraints and geodynamic concepts, *Geological Society special publication*, *179*(1), 337–354, doi: http://doi.org/10.1144/gsl.sp.2000.179.01.20.

Franke, W., R. D. Dallmeyer, and K. Weber (1995), Geodynamic Evolution, in *Pre-Permian Geology of Central and Eastern Europe*, edited by R. D. Dallmeyer, W. Franke, and K. Weber, pp. 579–593, Springer Berlin Heidelberg, Berlin, Heidelberg, doi: http://doi.org/10.1007/978-3-642-77518-5_57.

Gabriel, G., D. Vogel, R. Scheibe, H. Lindner, R. Pucher, T. Wonik, and C. M. Krawczyk (2011), Anomalies of the Earth's total magnetic field in Germany - the first complete homogenous data set reveals new opportunities for multiscale geoscientific studies: Magnetic anomalies in Germany, *Geophysical journal international*, *184*(3), 1113–1118, doi: http://doi.org/10.1111/j.1365-246x.2010.04924.x.

Gandl, J. (1998), Neue Daten zum jüngeren Paläozoikum Nordost-Bayerns und angrenzender Gebiete – Faziesentwicklung und geotektonische Konsequenzen,

*Geologica Bavarica*, *103*, 19–272.

Gräbe, R., and K. Wucher (1967), Schüttungs- und Strömungsrichtungen im Kulm des SE-Teils der Ziegenrücker Mulde (Ostthüringisches Schiefergebirge), *Geologie mediterraneenne*, *16*, 991–1006.

Hahn, T., U. Kroner, and P. Mezer (2010), Lower Carboniferous synorogenic sedimentation in the Saxo-Thuringian Basin and the adjacent Allochthonous Domain, in *Pre-Mesozoic geology of Saxo-Thuringia*, edited by U. Linnemann and R. L. Romer, pp. 171–192, Schweizerbart, Stuttgart.

Hallas, P., J. A. Pfänder, U. Kroner, and B. Sperner (2021), Microtectonic control of 40Ar/39Ar white mica age distributions in metamorphic rocks (Erzgebirge, N-Bohemian Massif): Constraints from combined step heating and multiple single grain total fusion experiments, *Geochimica et cosmochimica acta*, *314*, 178–208, doi: http://doi.org/10.1016/j.gca.2021.08.043.

Helmkampf, K. (2006), Profilvergleich und sedimentologische Entwicklung im Umkreis der Forschungsbohrungen Spitzeichen 1 und Lindau 1, *Geologica Bavarica*, *109*, 63–94.

Hofmann, Y. (2003), Gravimetrische und geodynamische Modellierungen in der Schwarmbeben-Region Vogtland/NW-Böhmen, Ph.D. thesis, Friedrich-Schiller-Universität Jena, Jena Germany.

Hofmann, Y., T. Jahr, and G. Jentzsch (2003), Three-dimensional gravimetric modelling to detect the deep structure of the region Vogtland/NW-Bohemia, *Journal of geodynamics*, *35*(1-2), 209–220, doi: http://doi.org/10.1016/s0264-3707(02)00063-7.

Hurich, C. A., and Y. Kristoffersen (1988), Deep structure of the Caledonide orogen in southern Norway: new evidence from marine seismic reflection profiling, *Special publication*.

Jouvent, M., O. Lexa, V. Peřestý, and P. Jeřábek (2022), New constraints on the tectonometamorphic evolution of the Erzgebirge orogenic wedge (Saxothuringian Domain, Bohemian Massif), *Journal of metamorphic geology*, *40*(4), 687–715, doi: http://doi.org/10.1111/jmg.12643.

Judersleben, G. (1972), Zur Petrologie des sedimentären Rotliegenden im Thüringer Wald und seinem Vorland, *Jb. Geol*, *4*, 181–289.

Juhlin, C., P. Hedin, D. G. Gee, H. Lorenz, T. Kalscheuer, and P. Yan (2016), Seismic imaging in the eastern Scandinavian Caledonides: siting the 2.5 km deep COSC-2 borehole, central Sweden, *Solid earth*, *7*(3), 769–787, doi: http://doi.org/10.5194/se-7-769-2016.

Kley, J., and T. Voigt (2008), Late Cretaceous intraplate thrusting in central Europe: Effect of Africa-Iberia-Europe convergence, not Alpine collision, *Geology*, *36*(11), 839–842, doi: http://doi.org/10.1130/G24930A.1.

Kossmat, F. (1927), Gliederung des varistischen Gebirgsbaues, *Abhandlungen des Sächsischen Geologischen Landesamtes*, *1*, 1–39.

Krawczyk, C. M., E. Stein, S. Choi, G. Oettinger, K. Schuster, H.-J. Götze, V. Haak, O. Oncken, C. Prodehl, and A. Schulze (2000), Geophysical constraints on exhumation mechanisms of high-pressure rocks: the Saxo-Thuringian case between the Franconian Line and Elbe Zone, *Geological Society special publication*, *179*(1), 303–322, doi: http://doi.org/10.1144/gsl.sp.2000.179.01.18.

Krohe, A. (1992), Structural evolution of intermediate-crustal rocks in a strike-slip and extensional setting (Variscan Odenwald, SW Germany): differential upward transport of metamorphic complexes and changing deformation mechanisms, *Tectonophysics*, *205*(4), 357–386, doi: http://doi.org/10.1016/0040-1951(92)90443-a.

Kroner, U., and R. L. Romer (2010), The Saxo-Thuringian Zone - tip of the Armorican Spur and part of the Gondwana plate, in *Pre-Mesozoic Geology of Saxo-Thuringia: From the Cadomian Active Margin to the Variscan Orogen*, edited by U. Linnemann and R. L. Romer, pp. 371–394, Schweizerbart, Stuttgart.

Kroner, U., and R. L. Romer (2013), Two plates — Many subduction zones: The Variscan orogeny reconsidered, *Gondwana research: international geoscience journal*, *24*(1), 298–329, doi: http://doi.org/10.1016/j.gr.2013.03.001.

Kroner, U., T. Hahn, R. L. Romer, and U. Linnemann (2007), The Variscan orogeny in the Saxo-Thuringian zone—Heterogenous overprint of Cadomian/Paleozoic Peri-Gondwana crust, in *The Evolution of the Rheic Ocean: From Avalonian-Cadomian Active Margin to Alleghenian-Variscan Collision*, vol. 31, edited by U. Linnemann, R. D. Nance, P. Kraft, and G. Zulauf, pp. 153–172, Geological Society of America, doi: http://doi.org/10.1130/2007.2423(06).

Kroner, U., J.-L. Mansy, S. Mazur, P. Aleksandrowski, H. P. Hann, H. Huckriede, F. Lacquement, J. Lamarche, P. Ledru, T. C. Pharaoh, H. Zedler, A. Zeh, and G. Zulauf (2008), Variscan tectonics, in *The Geology of Central Europe Volume 1: Precambrian and Palaeozoic*, edited by T. McCann, pp. 599–664, The Geological Society of London, London, doi: http://doi.org/10.1144/cev1p.11.

Kroner, U., M. Roscher, and R. L. Romer (2016), Ancient plate kinematics derived from the deformation pattern of continental crust: Paleo- and Neo-Tethys opening coeval with prolonged Gondwana–Laurussia convergence, *Tectonophysics*, *681*, 220–233, doi: http://doi.org/10.1016/j.tecto.2016.03.034.

Kroner, U., T. Stephan, and R. L. Romer (2022), Paleozoic orogenies and relative plate motions at the sutures of the Iapetus-Rheic Ocean, in *New Developments in the Appalachian-Caledonian-Variscan Orogen*, vol. 554, edited by Y. D. Kuiper, J. B. Murphy, R. D. Nance, R. A. Strachan, and M. D. Thompson, pp. 1–23, Geological Society of America, doi: http://doi.org/10.1130/2021.2554(01).

Kröner, A., P. Jaeckel, T. Reischmann, and U. Kroner (1998), Further evidence for an early Carboniferous ( 340 Ma) age of high-grade metamorphism in the Saxonian granulite complex, *Geologische Rundschau: Zeitschrift für allgemeine Geologie*, *86*(4), 751–766, doi: http://doi.org/10.1007/pl00009939.

Kylander-Clark, A. R. C., B. R. Hacker, and J. M. Cottle (2013), Laser-ablation split-stream ICP

petrochronology, *Chemical geology*, *345*, 99–112, doi: http://doi.org/10.1016/j.chemgeo.2013.02.019.

Köhler, S., F. Duschl, H. Fazlikhani, D. Koehn, T. Stephan, and H. Stollhofen (2022), Reconstruction of cyclic Mesozoic–Cenozoic stress development in SE Germany using fault-slip and stylolite inversion, *Geological magazine*, *159*(11-12), 1–23, doi: http://doi.org/10.1017/s0016756822000656.

Linnemann, U. (2007), Ediacaran rocks from the Cadomian basement of the Saxo-Thuringian Zone (NE Bohemian Massif, Germany): age constraints, geotectonic setting and basin development, *Geological Society special publication*, *286*(1), 35–51, doi: http://doi.org/10.1144/sp286.4.

Linnemann, U., N. J. McNaughton, R. L. Romer, M. Gehmlich, K. Drost, and C. Tonk (2004), West African provenance for Saxo-Thuringia (Bohemian Massif): Did Armorica ever leave pre-Pangean Gondwana? ? U/Pb-SHRIMP zircon evidence and the Nd-isotopic record, *International journal of earth sciences*, *93*(5), 683–705, doi: http://doi.org/10.1007/s00531-004-0413-8.

Linnemann, U., M. Hofmann, R. L. Romer, and A. Gerdes (2010), Transitional stages between the Cadomian and Variscan orogenies: Basin development and tectono-magmatic evolution of the southern margin of the Rheic Ocean in the Saxo-Thuringian Zone (North Gondwana shelf), in *Pre-Mesozoic geology of Saxo-Thuringia*, edited by U. Linnemann and R. L. Romer, pp. 59–98, Schweizerbart, Stuttgart.

Linnemann, U., M. Zweig, M. Zieger-Hofmann, T. Vietor, J. Zieger, J. Haschke, A. Gärtner, K. Mende, R. Krause, and F. Knolle (2024), The Harz Mountains (Germany) – Cadomia meets Avalonia and Baltica: U–Pb ages of detrital and magmatic zircon as a key for the decoding of Pangaea's central suture, *Geological Society special publication*, *542*(1), 403–431, doi: http://doi.org/10.1144/sp542-2023-52.

Massonne, H. J. (Ed.) (1998), *A new occurrence of microdiamonds in quartzofeldspathic rocks of the Saxonian Erzgebirge, Germany, and their metamorphic evolution*.

Matte, P. (1986), Tectonics and plate tectonics model for the Variscan belt of Europe, *Tectonophysics*, *126*(2-4), 329–374, doi: http://doi.org/10.1016/0040-1951(86)90237-4.

Mingram, B. (1998), The Erzgebirge, Germany, a subducted part of northern Gondwana: geochemical evidence for repetition of early Palaeozoic metasedimentary sequences in metamorphic thrust units, *Geological magazine*, *135*(6), 785–801, doi: http://doi.org/10.1017/s0016756898001769.

Oncken, O. (1998), Evidence for precollisional subduction erosion in ancient collisional belts: The case of the Mid-European Variscides, *Geology*, *26*(12), 1075–1078, doi: http://doi.org/10.1130/0091-7613(1998)026<1075:EFPSEI>2.3.CO;2.

Ravidà, D. C. G. (2023), Novel approaches to the continental Permian-Triassic successions in southeast Germany, Ph.D. thesis, Friedrich-Alexander-Universität Erlangen-Nürnberg (FAU).

Reh, H. (1954), Die Mineralquellen des Bades Liebenstein in Thüringen, *Geologie mediterraneenne*, *3*(6), 7.

Reinhardt, J., and U. Kleemann (1994), Extensional unroofing of granulitic lower crust and related low-pressure, high-temperature metamorphism in the Saxonian Granulite Massif, Germany, *Tectonophysics*, *238*(1-4), 71–94, doi: http://doi.org/10.1016/0040-1951(94)90050-7.

Richter, G. (1941), Paläogeographische und tektonische Stellung des Richelsdorfer Gebirges im hessischen Raum, *Jb. Reichsst. Bodenforsch*, *61*, 283–332.

Ritter, O., V. Haak, V. Rath, E. Stein, and M. Stiller (1999), Very high electrical conductivity beneath the Münchberg Gneiss area in Southern Germany: implications for horizontal transport along shear planes, *Geophysical journal international*, *139*(1), 161–170, doi: http://doi.org/10.1046/j.1365-246X.1999.00937.x.

Robardet, M. (2002), Alternative approach to the Variscan Belt in southwestern Europe: Preorogenic paleobiogeographical constraints, in *Variscan-Appalachian dynamics: The building of the late Paleozoic basement*, vol. 364, edited by J. R. M. Catalán, Hatcher, Robert D., Jr., R. Arenas, and F. D. García, pp. 1–15, Geological Society of America, doi: http://doi.org/10.1130/0-8137-2364-7.1.

Romer, R. L., and U. Kroner (2022), Provenance control on the distribution of endogenic Sn-W, Au, and U mineralization within the Gondwana-Laurussia plate boundary zone, in *New Developments in the Appalachian-Caledonian-Variscan Orogen*, vol. 554, edited by Y. D. Kuiper, J. B. Murphy, R. D. Nance, R. A. Strachan, and M. D. Thompson, pp. 25–46, Geological Society of America, doi: http://doi.org/10.1130/2021.2554(02).

Romer, R. L., U. Kroner, C. Schmidt, and C. Legler (2022), Mobilization of tin during continental subduction-accretion processes, *Geology*, *50*(12), 1361–1365, doi: http://doi.org/10.1130/g50466.1.

Rötzler, J., and R. L. Romer (2001), P–T–t evolution of ultrahigh-temperature granulites from the Saxon granulite massif, Germany. Part I: Petrology, *Journal of petrology*, *42*(11), 1995–2013, doi: http://doi.org/10.1093/petrology/42.11.1995.

Rötzler, K., and B. Plessen (2010), The Erzgebirge: a pile of ultrahigh-to low-pressure nappes of Early Palaeozoic rocks and their Cadomian basement, *Pre-Mesozoic geology of Saxo-Thuringia: From the Cadomian active margin to the Variscan orogen*, pp. 253–270.

Scherer, E. E., K. Mezger, and C. Münker (2002), Lu-Hf ages of high-pressure metamorphism in the Variscan fold belt of southern Germany, *Geochimica et Cosmochimica Acta*, *66*(Supplement 1), A677.

Schmädicke, E., M. Okrusch, and W. Schmidt (1992), Eclogite-facies rocks in the Saxonian Erzgebirge, Germany: high pressure metamorphism under contrasting P-T conditions, *Contributions to mineralogy and petrology. Beitrage zur Mineralogie und Petrologie*, *110*(2-3), 226–241, doi: http://doi.org/10.1007/bf00310740.

Schulmann, K., J.-B. Edel, J. R. Martínez Catalán, S. Mazur, A. Guy, J.-M. Lardeaux, P. Ayarza, and I. Palomeras (2022), Tectonic evolution and global crustal architecture of the European Variscan belt constrained by geophysical data, *Earth-science reviews*, *234*(104195), 104,195, doi:

http://doi.org/10.1016/j.earscirev.2022.104195.

Schulz, B., and J. Krause (2024), Electron probe petrochronology of monazite- and garnet-bearing metamorphic rocks in the Saxothuringian allochthonous domains (Erzgebirge, Granulite and Münchberg massifs), *Geological Society special publication*, *537*(1), 249–284, doi: http://doi.org/10.1144/sp537-2022-195.

Schust, F., W. Busch, and W. Gotte (2000), Uber die Metamorphite der Brg. Schleusingen 3/63 (Sudthuringen) und ihre geologische Position, *Zeitschrift für geologische Wissenschaften*, *28*(3/4), 381–396.

Schäfer, F., O. Oncken, H. Kemnitz, and R. L. Romer (2000), Upper-plate deformation during collisional orogeny: a case study from the German Variscides (Saxo-Thuringian Zone), *Geological Society special publication*, *179*(1), 281–302, doi: http://doi.org/10.1144/gsl.sp.2000.179.01.17.

Skiba, P., G. Gabriel, D. Vogel, C. Krawczyk, and C. Vinnemann (2010), Bouguer anomaly map of Germany.

Stamm, R., and F. Goerlich (1988), Das Grundgebirge der Süddeutschen Grossscholle, *Zentralblatt für Geologie und Paläontologie, Teil 1: Allgemeine, Angewandte, Regionale und Historische Geologie*, *1987*(11-12), 1403–1439.

Stephan, T., U. Kroner, T. Hahn, P. Hallas, and T. Heuse (2016), Fold/cleavage relationships as indicator for late Variscan sinistral transpression at the Rheno-Hercynian–Saxo-Thuringian boundary zone, Central European Variscides, *Tectonophysics*, *681*, 250–262, doi: http://doi.org/10.1016/j.tecto.2016.03.005.

Stephan, T., U. Kroner, R. L. Romer, and D. Rösel (2019), From a bipartite Gondwanan shelf to an arcuate Variscan belt: The early Paleozoic evolution of northern Peri-Gondwana, *Earth-science reviews*, *192*, 491–512, doi: http://doi.org/10.1016/j.earscirev.2019.03.012.

Stettner, G., and M. Salger (1985), Das Schiefergebirge in der Forschungsbohrung Obernsees, *Geologica Bavarica*, *88*, 49–55.

Talwani, M. (1973), Computer usage in the computation of gravity anomalies, in *Methods in Computational Physics: Advances in Research and Applications*, vol. 13, edited by B. A. Bolt, pp. 343–389, Elsevier, doi: http://doi.org/10.1016/b978-0-12-460813-9.50014-x.

Thieme, M., F. Jähne-Klingberg, B. Fügenschuh, U. Linnemann, A. Malz, and K. Ustaszewski (2023), The Late Mesozoic to Palaeogene cooling history of the Thuringian Forest basement high and its southern periphery (Central Germany) revealed by combined fission-track and U-Pb LA-ICP-MS dating, *Zeitschrift der Deutschen Gesellschaft für Geowissenschaften*, *174*(3), 593–612, doi: http://doi.org/10.1127/zdgg/2023/0321.

Tichomirowa, M., S. Sergeev, H.-J. Berger, and D. Leonhardt (2012), Inferring protoliths of high-grade metamorphic gneisses of the Erzgebirge using zirconology, geochemistry and comparison with lower-grade rocks from Lusatia (Saxothuringia, Germany), *Contributions to mineralogy and petrology. Beitrage zur Mineralogie und Petrologie*, *164*(3), 375–396, doi: http://doi.org/10.1007/s00410-012-0742-8.

Trusheim, F. (1964), Über den Untergrund Frankens; Ergebnisse von Tief Bohrungen in Franken und Nachbargebieten, *Geologica Bavarica*, *54*, 1–106.

von Gaertner, H. R. (1951), Probleme des Saxothuringicums, *Geologische Rundschau: Zeitschrift für allgemeine Geologie*, pp. 409–450.

Wiest, J. D., S. Köhler, D. Koehn, H. Stollhofen, K. Dengler, and H. Fazlikhani (2025), A novel multi-scale approach to fault network analysis and visualization: test case Franconian Platform (SE Germany), *Journal of structural geology*, *199*(105481), 105,481, doi: http://doi.org/10.1016/j.jsg.2025.105481.

Will, T. M. (2001), Paleostress-tensor analysis of late deformation events in the Odenwald Crystalline Complex and comparison with other units of the Mid-German Crystalline Rise, Germany, *Mineralogy and petrology*, *72*(1-3), 229–247, doi: http://doi.org/10.1007/s007100170035.

Will, T. M., E. Schmädicke, X.-X. Ling, X.-H. Li, and Q.-L. Li (2021), Geochronology, geochemistry and tectonic implications of Variscan granitic and dioritic rocks from the Odenwald-Spessart basement, Germany, *Lithos*, *404-405*(106454), 106,454, doi: http://doi.org/10.1016/j.lithos.2021.106454.

Willner, A. P., A. Krohe, and W. V. Maresch (2000), Interrelated PTtd paths in the Variscan Erzgebirge dome (Saxony, Germany): Constraints on the rapid exhumation of high-pressure rocks from the root zone of a collisional orogen, *International geology review*, *42*(1), 64–85.

Wunderlich, J. (1989), New results on the geology of the southeastern Ruhla Crystalline Complex, *Freiberger Forschungshefte, Reihe C*, *429*, 7–32.

Wurm, A. (1926), Über den Bauplan des variskischen Gebirges am Westrand der Böhmischen Masse, *Geologische Rundschau*, *17*(4), 241–257, doi: http://doi.org/10.1007/bf01801780.

Wurm, A. (1929), *Die Nürnberger Tiefbohrungen: ihre wissenschaftliche und praktische Bedeutung*, Bayerisches Oberbergamt.

Wurm, A. (1961), *Frankenwald, Münchberger Gneismasse, Fichtelgebirge, Nördlicher Oberpfälzer Wald*, Geologie von Bayern, 2 ed., Borntraeger, Stuttgart, Germany.

Zeh, A., and T. M. Will (2010), The mid-German crystalline zone, *Pre-Mesozoic Geology of Saxo-Thuringia—From the Cadomian Active Margin to the Variscan Orogen. Schweizerbart, Stuttgart*, pp. 195–220.

Ziegenhardt, W., and J. Jungwirth (1972), Erläuterungen zur Geologischen Spezialkarte der DDR 1 : 25 000, Bl. Plaue 5231. - 269 S.